UCRL 569

Cy. 2

UNIVERSITY OF CALIFORNIA

Radiation Laboratory

TWO-WEEK LOAN COPY

This is a Library Circulating Copy which may be borrowed for two weeks. For a personal retention copy, call Tech. Info. Division, Ext. 5545

BERKELEY, CALIFORNIA

DISCLAIMER

This document was prepared as an account of work sponsored by the United States Government. While this document is believed to contain correct information, neither the United States Government nor any agency thereof, nor the Regents of the University of California, nor any of their employees, makes any warranty, express or implied, or assumes any legal responsibility for the accuracy, completeness, or usefulness of any information, apparatus, product, or process disclosed, or represents that its use would not infringe privately owned rights. Reference herein to any specific commercial product, process, or service by its trade name, trademark, manufacturer, or otherwise, does not necessarily constitute or imply its endorsement, recommendation, or favoring by the United States Government or any agency thereof, or the Regents of the University of California. The views and opinions of authors expressed herein do not necessarily state or reflect those of the United States Government or any agency thereof or the Regents of the University of California.

UCRL 569

UNCLASSIFIED

cy 2

A Study of Protons Ejected from Nuclei by High Energy Gamma - Rays

By

Cyrus Levinthal
A.B. (Swarthmore College) 1943

DISSERTATION

Submitted in partial satisfaction of the requirements for the degree of

DOCTOR OF PHILOSPHY

in

Physics

in the

GRADUATE DIVISION

of the

UNIVERSITY OF CALIFORNIA

Approved:

. . . . . .

. . . . . .

. . . . . .

Committee in Charge

Deposited in the University Library . . . . . .
Date Librarian

UNCLASSIFIED

Table of Contents

		Page Number
I	Introduction	1
II	General Experimental Method	6
III	Apparatus	9
	Counters	9
	Electronics	12
IV	Arrangement of Components	14
V	Experimental Checks	16
VI	Calculations and Corrections	23
VII	Results and Discussion	27
VIII	Acknowledgements	32
IX	Bibliography	33

Omissions:

P. 2	(middle)	with an energy $\underline{\varepsilon}$
	(bottom)	energy $\underline{\varepsilon}$ from a nucleus.
P. 7	(near top)	two equs. of from of (5) fro $\underline{I_1}$ and I_2
		cross out "unk"
	(near bottom)	if we measure $\frac{\Delta I}{I}$
	(near bottom)	$\frac{\Delta I}{I} = \frac{(R)^{-.44} - (R + \Delta R)^{-.44}}{(R + \Delta R)^{-.44}}$
P. 18	(near bottom)	counter #1, counter # 2 - - - -
		coincidence circuit resp.
P. 24	(top)	$\frac{d\sigma\ (E,\theta)}{dE\ d\Omega}$ ←
P. 28	(bottom)	, and β is the vel. of proton.
P. 29	(bottom)	non-adiabatic

UNCLASSIFIED

I Introduction.

The fact that gamma rays (that is high energy x-radiation) cause nuclear reactions has been known for several years. In 1935, Chadwick and Goldhaber[1] demonstrated the photo-disintegration of the deuteron using gamma rays from Th C^{11}. The products of these reactions have been studied using the gamma rays of such radioactive nuclei as Na^{24}, Mn^{56}, Ga^{72}, La^{140} whose energies are 2.76, 2.7, 1.5, and 2.5 Mev respectively.[2] The 17 Mev gamma rays from the Li^7 (p, γ) reaction have been used extensively by several groups.[3]

With the construction of high energy electron accelerators such as betatrons and synchrotrons this work has been extended to the higher energy regions. The General Electric group[4] used the 100 Mev betatron, and studies are now in progress in this laboratory using the beam from the 335 Mev synchrotron.

Most of the experiments referred to have been studies of the radioactive end products of various reactions, so that the total cross sections were obtained for (γ, η), (γ, p), $(\gamma, 2\eta)$ etc, reactions with various energy gamma rays on different elements. It has been found that at least up to 100 Mev the most probable reaction is one in which only a single particle is emitted.[4] In the case of carbon, copper and tantalum the (γ, n) reaction appears to have a very pronounced maximum for gamma rays between 20 and 30 Mev.

In order to understand the possible mechanisms in these reactions it is first necessary to consider some of the proposals which have been made about nuclear reactions in general. The concept which has been most useful in dealing with heavy particle induced reactions below about 50 Mev is that of the compound nucleus. This idea, introduced by Bohr[5] in 1935, is based on the strong nucleon-nucleon interaction in the nucleus. It is

assumed that if a neutron, for example, impinges on a nucleus, then by successive collisions within the nucleus its energy is distributed among all the nucleons. Thus a compound nucleus is formed of the original target nucleus plus the incident particle. Since no one particle now has enough energy to overcome its binding, the compound nucleus lasts for a time long compared to the time of a nucleon's flight across the nucleus, i.e. long compared to 10^{-21} sec. Finally a particle will accumulate the necessary energy to escape and it will "boil out". This disintegration will continue by successive evaporation of particles until the available energy is less than the binding energy of any particle.

Using these ideas we can analyze a nuclear reaction in two parts: first, the absorption of the incident particle α to form the compound nucleus, the cross section for this process we call $\sigma_\alpha(c)$; second, the possibility $\eta_\beta(\varepsilon)$ of the emission of a particle β with an energy ε. The fundamental idea of the compound nucleus is that we can write the total cross section for the process

$$\sigma(\alpha,\beta) = \sigma_\alpha(c)\,\eta_\beta(\varepsilon) \qquad (1)$$

A method of dealing with the evaporation process has been discussed by Weisskopf[6]. He uses the principle of detailed balance between the emission of a particle from the compound nucleus and the absorption of this particle. In this way the probability of the emission of a particle of energy ε from a nucleus excited to an energy E is found to be

$$I(\varepsilon) = K\varepsilon\,\frac{\omega(E-\varepsilon-B_\beta)}{\omega(E)}\,\sigma_\beta(\varepsilon) \qquad (2)$$

where $\omega(E)$ is the level density of the nucleus at the energy E, before the emission; $\omega(E-\varepsilon-E_b)$ is the level density of the residual nucleus after a particle with a binding energy E_b has been emitted with a kinetic energy ε; and $\sigma\beta(\varepsilon)$ is the capture cross section of the residual nucleus for the particle β. The functional form of the level density depends on the model one takes to represent the nucleus. But most models proposed, for instance both the liquid drop and the Fermi gas, give

$$\omega(E) = Ce^{-aE^n} \tag{3}$$

where n is close to 1/2.

For neutrons and protons, the capture cross section can be computed to reasonable accuracy.[7] Using these results in Equations (1) and (2), we can calculate the cross section for the emission of any particle in a reaction induced by heavy particles.

The problem is immediately made more difficult in the case of gamma ray induced reactions since we do not know the probability that they will excite the compound nucleus. However, if the picture of the compound nucleus is at all applicable to gamma ray processes there are some conclusions that can be drawn. The relative probability of two reactions such as (γ,p) and (γ,n) can be calculated with no assumptions as to the probability of excitation by the gamma ray. This ratio involves only the integral of Equation (2) over the energy region available in the two cases. The ratio of (γ,p) to (γ,n) calculated in this way for 17 Mev gammas can be compared with the experimental results of Hirtzel and Wäffler[8] who used the Li (p,γ) reaction to produce monoenergetic gammas. The calculated results for the ratio are of the order of a factor of 100 lower than the observed results.

Shiff[9] attempted to explain the experimental results by assuming that the gamma rays can excite only a few of the nuclear energy levels, and that the density of these levels is a very slowly varying function of the energy.

Goldhaber and Teller[10] have discussed nuclear dipole vibrations in connection with the observations of Baldwin and Klaiber[11] that (γ,n) reactions have rather sharp maxima for γ's of about 20 Mev. This work considers the volume and surface vibrations of the protons with respect to the neutrons. It is shown that there would be a resonance for these vibrations at about 20 Mev so that the observed maxima would then correspond to a high probability of formation of the compound nucleus.

There is one more approach which has been used to explain some gamma ray induced reactions. One can consider the action of the electromagnetic field of the photon on a single particle in the nucleus. This type of calculation is analagous to that used for the photoelectric effect of electrons in an atom[12]. The calculations have been done for the photo-disintegration of the deuteron[13,14] and for Be^9 [15], but no attempt has been made to use these concepts for the photo-reactions in heavy elements.

In considering experiments done with the gamma ray beam from an electron accelerator, the spectral distribution of the photons must be kept in mind. The synchrotron accelerates electrons to a maximum energy of 335 Mev, and then allows them to strike a 0.020 inch platinum target. When the electrons are accelerated by the coulomb field of the platinum atoms they radiate gamma rays. The Bremsstrahlung (continuous gamma ray) spectrum is approximately such that the number of quanta per unit energy is inversely proportional to the energy up to a maximum of 335 Mev.

These experiments were undertaken in the hope that they might help explain the mechanism of gamma ray induced reactions. With this in mind the energy distribution of the protons ejected by the synchrotron beam from carbon, copper, and lead was studied. An angular distribution of the protons at one energy was made with targets of carbon and copper. And an attempt was made to determine the absolute value of the cross section for these processes.

II General Experimental Method.

The main problem in this experiment was to count protons and measure their range. Fundamentally, the procedure used was the measurement of the specific ionization of particles at two points along their path. If we consider the energy loss formula of Bethe[16] we can write

$$\frac{dE}{dX} = K Z^2 f(v) = I = \text{specific ionization} \qquad (1)$$

where $\frac{dE}{dX}$ is the energy loss due to ionization per unit length of path; Z is the charge of the ionizing particle in units of the electron charge; f(v) is a function of the velocity of the particle only; and K is a constant dependant only on the properties of the stopping material. We can rewrite this as

$$\frac{dE}{dX} = K Z^2 F'\left(\frac{E}{m}\right) \qquad (2)$$

If Equation (2) is integrated from zero energy to an energy E corresponding to a range R, we have

$$R = \frac{K m}{Z^2} F\left(\frac{E}{m}\right) \qquad (3)$$

An exact numerical integration of the energy loss equation up to one hundred Mev shows that for stopping materials in the middle of the periodic table we can write[17]

$$R = K' \frac{m}{Z^2} \left(\frac{E}{m}\right)^{1.8} \qquad (4)$$

Therefore

$$I = \frac{dE}{dX} = K'' Z^2 \left(\frac{m}{R}\right)^{.445} \qquad (5)$$

This approximation is valid down to about 2 Mev for protons.

If we measure I at two points separated by a known thickness of stopping material, we have I_1 at R, and I_2 at R plus ΔR. Thus with the two equations of the form of (5) for I and I_1 we can solve for the two unknowns R and m. In principle this process can be carried to any desired degree of precision but in this experiment several simplifications were made.

We shall designate the first counter entered by the particle as the front, and the second as the back counter. If we accept in the back counter only very large pulses this means that the initiating particle is near the end of its range. Let us assume, for the moment, that the particles being measured are all protons. We can determine the range interval accepted in the back counter by examining the pulse height distribution in the front counter. Figure II-(1) illustrates this point. In the back counter we accept all pulses corresponding to dE/dX greater than A. Then the pulse height analysis in the front counter should give $\Delta I/I$, in the example shown of 19 percent. The inverse of this can of course also be done. If we measure $\Delta I/I$, and know ΔR, the value of R can be found from the curve. If the apprximation of Equation (4) is valid we can write

$$\frac{\Delta I}{I} = \frac{I_1 - I_2}{I_2} = \frac{(\Delta R)^{-.44} - (R + \Delta R)^{-.44}}{(R + \Delta R)^{-.44}}$$

$$\text{or} \quad \frac{\Delta I}{I} = \left(\frac{R + \Delta R}{\Delta R}\right)^{.44} - 1$$

$$\text{or} \quad R = \Delta R \left[\left(\frac{\Delta I}{I} + 1\right)^{2.24} - 1\right] \qquad (6)$$

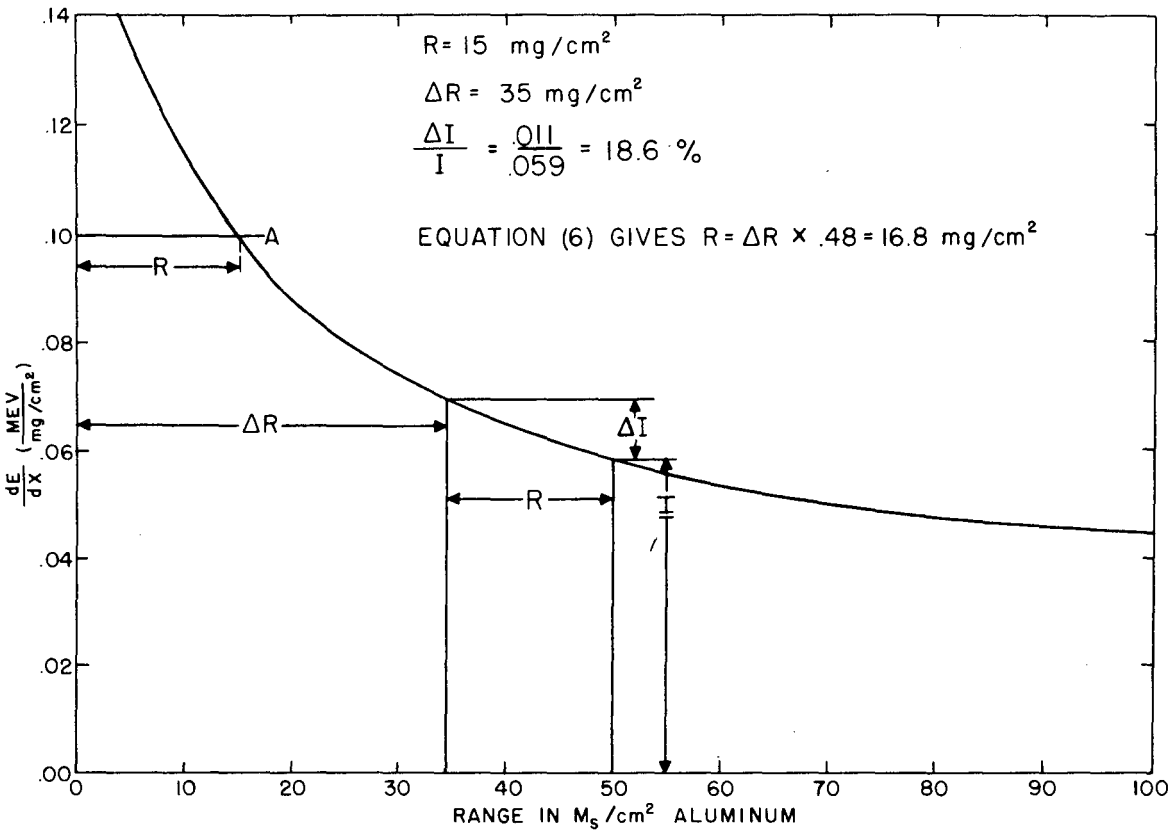

FIG. II—(1)

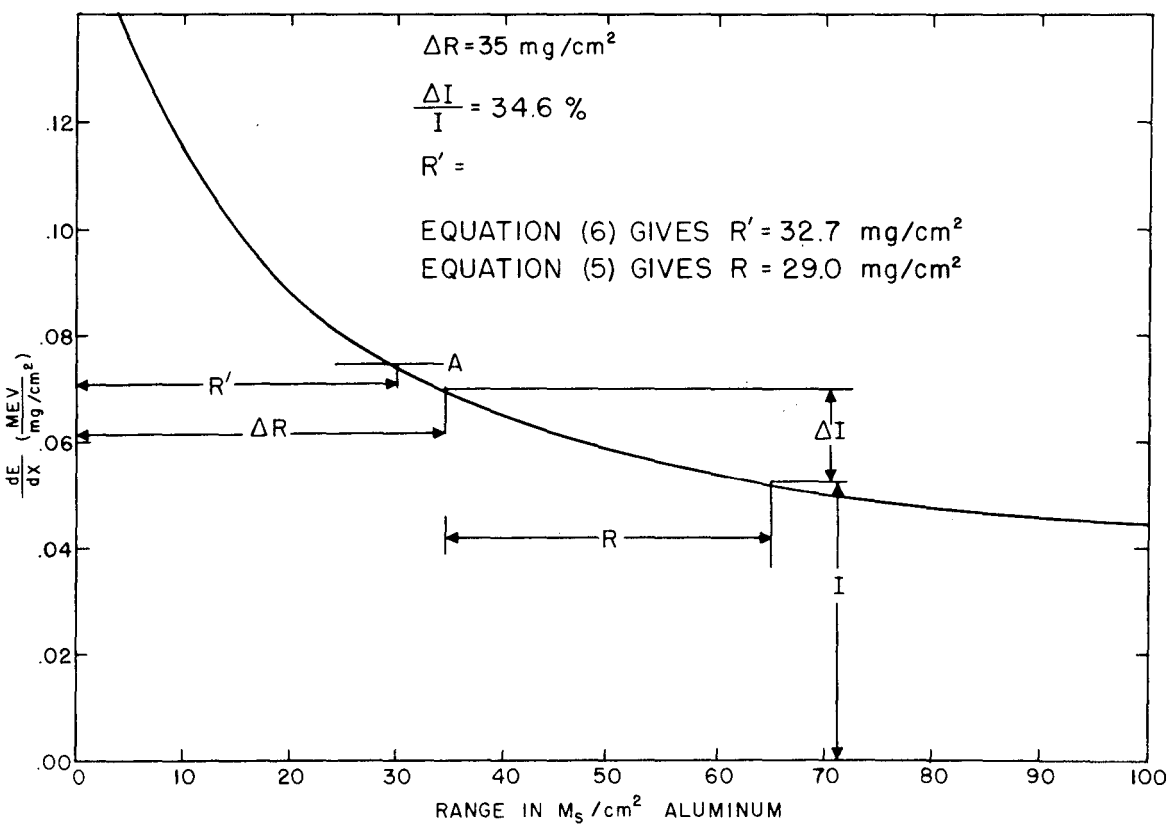

FIG. II—(2)

14463-2

In this way we determine the equivalent range interval that is accepted by the back counter. The calculation can be checked by changing the discrimination on the back counter by a given amount--say to 75 percent. Then from Equation (5) the range R should change by a factor of .75 raised to the 2.24 power. From Equation (6) or from a graphical analysis as in Figure II-(2) the new value Δ^{I}/I can be computed and compared with the measured result. If this check is satisfactory it can be concluded that we are actually dealing with only one kind of particle as was assumed.

Another check which can be made of this latter assumption is to increase the amount of material ΔR between the counters and again measure the pulse height distribution. Since Δ^{I}/I is now small, different kinds of particles would show up as two or more different peaks in the pulse height distribution.

III Apparatus

Counters

As stated above, the basis of these experiments is a measurement of the rate of energy loss of a particle at two points along its path. Particles moving with non-relativistic velocities, i.e. much less than the velocity of light, lose their energy by collision with, and ionization of the matter through which they pass. Thus it is only necessary to measure the ionization produced in a thin region to know the rate of energy loss of the particle. This was done by means of proportional gas counters since their operation has been studied rather extensively and their output is known to be proportional to the ionization over very wide limits.

A proportional counter is essentially a vessel filled with gas and containing a thin wire held at a positive voltage with respect to the walls. Electrons which are liberated in the original ionization drift toward the wire and if they receive sufficient energy from the electric field they produce secondary ions in the gas. The secondary electrons thus produced also drift toward the wire and eventually all are collected on it. The motion of the electrons and the positive ions induces a charge on the wire causing a drop in its voltage which then can be amplified and measured.

In the low field region far from the wire electrons gain energy very slowly, making thousands of collisions with gas molecules before gaining one electron volt. In this region it is much more probable that they finally lose their energy by raising a molecule to an excited

electronic state rather than ionizing it. If however the electric field gradient is sufficiently high, electrons will gain the energy necessary to cause ionization in a few mean free paths, so that in such a region ionization will take place. In a proportional counter the voltage is adjusted so that secondary ions are formed only very close to the wire, say within a few thousands of an inch. Thus the multiplication remains finite and does not cause a complete electrical discharge as in the case of a Geiger counter. A counter operated in this region will be truly proportional provided a) that recombination of electrons with ions or electron attachment to neutral molecules is negligible and b) that the space charge due to the electrons near the wire does not excessively distort the electric field. It has been found experimentally by the Los Alamos workers[18] that a) is satisfied for most of the common gasses, even for very heavily ionizing particles. However, the space charge effect will of course become important if sufficient ionization takes place in the counter. Corson and Wilson[19] have shown that the effect is negligible if the energy lost per centimeter in the counter (in electron volts) multiplied by the gas multiplication is less than 10^9. This is only a very rough rule of thumb, since the space charge effect is strongly dependent upon the path of the primary particle. It does indicate however, that in the present case the problem is nonexistent, since the above quantity was never more than 10^7.

By considering the momentum balance for electrons in a unit volume of the gas, the problem of the diffusion of electrons in an electric field can be solved. The result given by Rossi and Staub[20] is that the drift velocity ω is given by the equation

$$\vec{\omega} = \frac{e}{m} \frac{\lambda}{u} \frac{\vec{E}}{p}$$

where e and m are the electronic charge and mass; λ is the mean free path of the electrons and u is their mean agitation velocity, $\vec{E}$ is the electric field strength and p the pressure. In argon the first excited state to which the electron can transfer its energy is at 11 e.v. so that the mean agitation velocity corresponds to about 9 e.v. At this energy the mean free path is very small. If a small quantity of CO_2 is added to the argon, the mean agitation energy is kept small by excitation of low-lying vibrational states. The additional effectiveness of the CO_2 can be seen from the data of Brode[21] which shows that the scattering cross section of electrons on argon goes almost to zero for low energies. Thus the mean free path will also be much longer if the electrons are kept at low agitation velocities. This explains the experimentally verified result that the drift velocity is considerably higher in an argon-CO_2 mixture than in either gas by itself.

A mixture of 95 percent Argon and 5 percent CO_2 was used in these counters. For this mixture, and at the voltages used, the drift velocity is about 6×10^6 centimeters/second. The protons were collimated so that their maximum distance from the wire was about 2 centimeters. Thus the delay before the gas multiplication started was less than 4×10^{-7} seconds. The counters were rectangular in shape with dimensions of 4-1/2 x 3 x 1-1/2 inches.

A 0.003 inch tungsten wire was centered along the major axis of the rectangle. It was terminated on one end by a silver solder bead and on the other by a number 18 copper wire with a solder connection. The solder bead was drilled and supported from the walls with a nylon string.

The copper wire was brought out of the counter through a Kover glass seal and was then connected to a high voltage supply and the input of the pre-amplifier. On the large faces of the counters flanges were mounted to support 2-1/2 inches dural foils. Thus we effectively have counters with a cylindrical active region of roughly 2-1/2 inch diameter and 2 inch depth.

Electronics.

(A block diagram of the equipment is shown in Figure III-(1).)

The general requirements of the electronics associated with the counters were 1) that they have a wide enough band width to pass the leading edge of the pulse from the counter; 2) that the response of all the circuits be linear, that is, that the output of the amplifiers be proportional to the input; 3) that the pulses into the discriminators must be as short as possible to avoid having several small pulses build up to resemble a large one; 4) that the pulses into the coincidence circuit must be as short as possible so that accidental coincidences between the counters could be reduced; 5) that the amplifier, pulse height discriminators, and the high voltage supply must be sufficiently stable so that there would be negligible drift over a period of several hours.

It was found that all of these requirements could be met to the degree demanded by these experiments by using for the most part standard components which had been designed and built by the Electronics group under the direction of H. Farnsworth. The pre-amplifiers were a modified version of those designed by Mr. Bruce Cork. They were made to fit directly

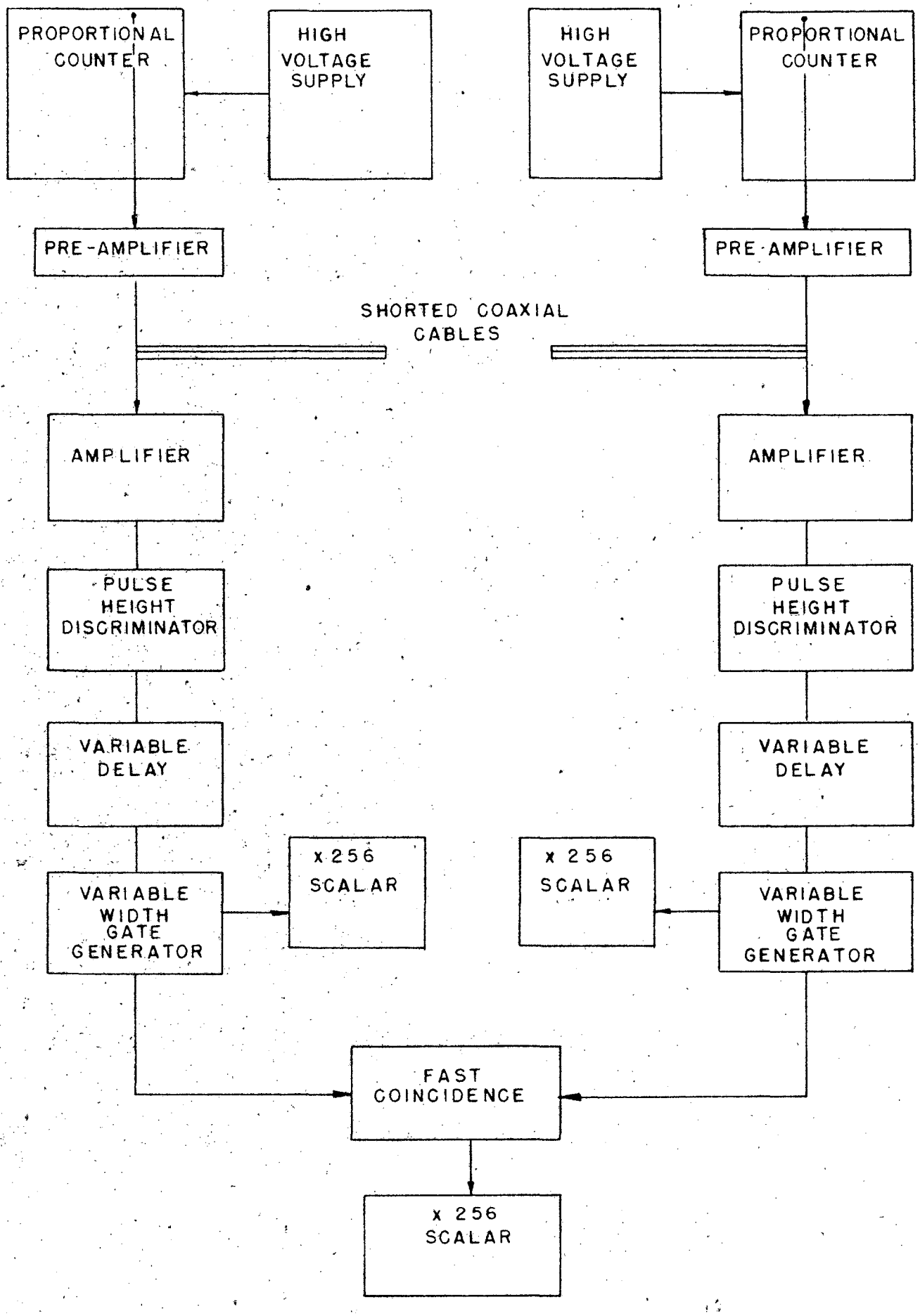
PROPORTIONAL COUNTER
HIGH VOLTAGE SUPPLY
HIGH VOLTAGE SUPPLY
PROPORTIONAL COUNTER
PRE-AMPLIFIER
PRE-AMPLIFIER
SHORTED COAXIAL CABLES
AMPLIFIER
AMPLIFIER
PULSE HEIGHT DISCRIMINATOR
PULSE HEIGHT DISCRIMINATOR
VARIABLE DELAY
VARIABLE DELAY
x 256 SCALAR
x 256 SCALAR
VARIABLE WIDTH GATE GENERATOR
VARIABLE WIDTH GATE GENERATOR
FAST COINCIDENCE
x 256 SCALAR

FIG. III (1)

on the counters with bananna plug connections and as used here had a gain of about 100, and a negative output. The output of the pre-amplifiers was delivered to the counting racks from the magnet room of the synchrotron via coaxial cables. At this point the signal was fed into high gain linear amplifiers (maximum gain 10,000). However, in parallel to the input of the linear amplifiers, there was a shorted coaxial cable 100 feet long which shaped the pulse into the linear amplifier, to about 4×10^{-7} seconds. The output of the linear amplifier went into the discriminator of a circuit which generated a gate of constant amplitude and variable width and variable delay. The width of this gate was set at 4×10^{-7} seconds and was then fed into a coincidence circuit.

For these experiments in which the pulse height distribution was wanted a 10 channel pulse height analyzer was used. This device was built by Clyde Weigand and W. Goldsworthy following the design of Dexter and Sands[22]. The pulse height analyzer needs an input pulse of 2×10^{-6} seconds to operate with maximum stability so that a longer shorted line was used at the input of its linear amplifier. In order to measure the height of only those pulses which were in time coincidence with pulses from the other counter, the register pulse of the analyzer was gated with the output of the first coincidence unit. A block diagram of the set-up with the pulse height analyzer is shown in Figure III-(2).

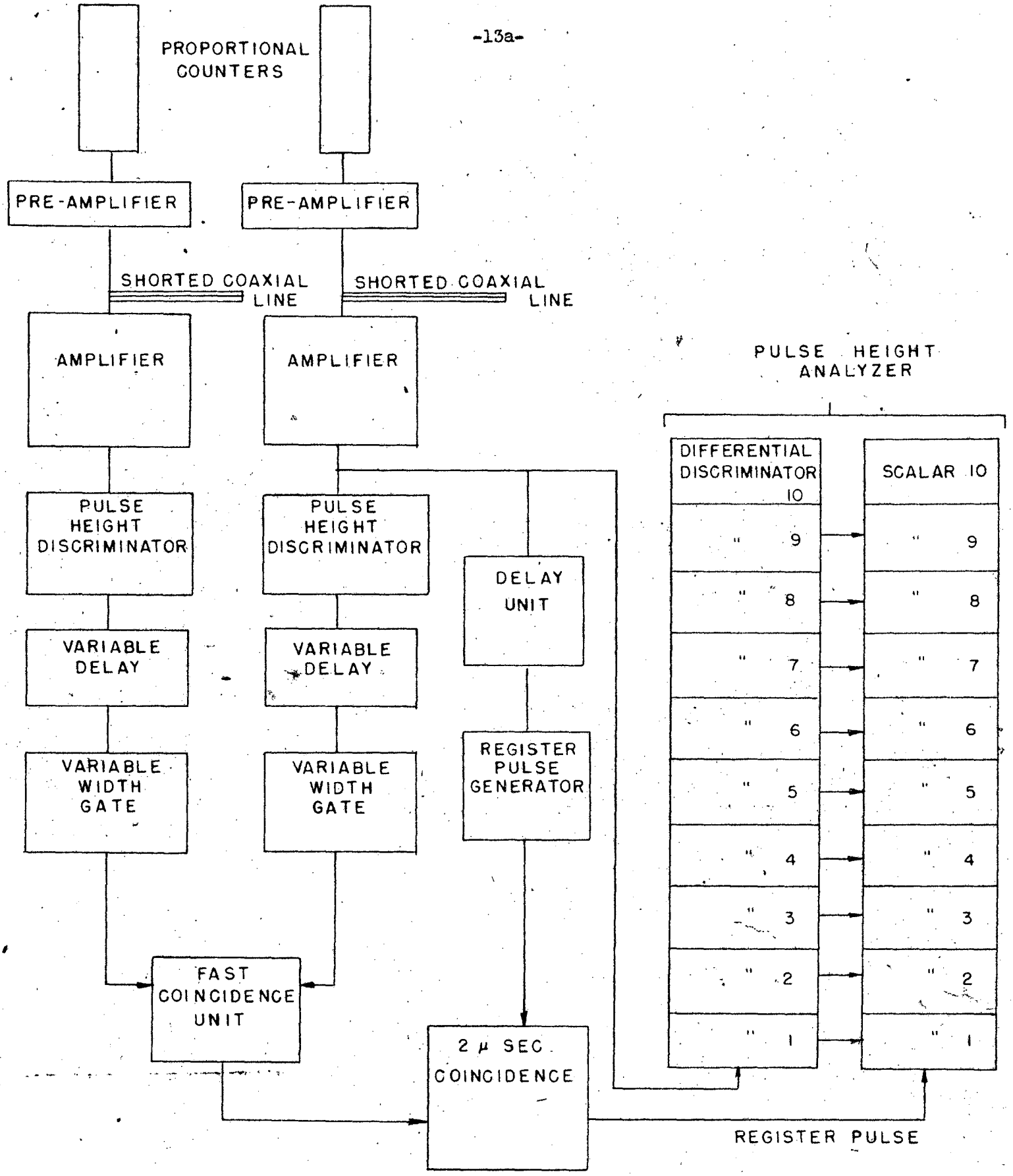
PROPORTIONAL COUNTERS
PRE-AMPLIFIER
PRE-AMPLIFIER
SHORTED COAXIAL LINE
SHORTED COAXIAL LINE
AMPLIFIER
AMPLIFIER
PULSE HEIGHT ANALYZER
PULSE HEIGHT DISCRIMINATOR
PULSE HEIGHT DISCRIMINATOR
DELAY UNIT
VARIABLE DELAY
VARIABLE DELAY
REGISTER PULSE GENERATOR
VARIABLE WIDTH GATE
VARIABLE WIDTH GATE
FAST COINCIDENCE UNIT
2 μ SEC COINCIDENCE
DIFFERENTIAL DISCRIMINATOR 10
" 9
" 8
" 7
" 6
" 5
" 4
" 3
" 2
" 1
SCALAR 10
" 9
" 8
" 7
" 6
" 5
" 4
" 3
" 2
" 1
REGISTER PULSE

FIG. III (2)

IV Arrangement of Components.

The arrangement of the targets and counter was quite simple as shown in Figure IV-(1). The targets were made 3 inches square and mounted on a holder centered directly below the beam. The target holder could be rotated and locked at any angle with respect to the beam. In most runs the front of the counter telescope was 6 inches from the target center. Directly in front of the counters was a collimating hole 1-1/4 inch in diameter, drilled in a 2 inch lead brick. At the back of this brick a 1/4 inch recess was milled so that absorbers could be placed immediately in front of the counter. The axes of the counters and the center of the collimator were aligned so that they pointed at the spot where the center of the beam struck the target. The entire counter system was surrounded by lead except on the top where the pre-amplifiers were connected. For the energy distributions, which were all taken with the counter axis at 90° to the beam, 2 inches of lead was placed under the counters and 4 inches on the sides. When the counters were rotated to other angles some of the lead on the sides had to be removed.

The counters, shielding and target holder were arranged on an aluminum plate which was bolted to a heavy metal stand. The center of the target holder was alighed with the beam axis by using a transit which was in turn aligned by taking photographs of the beam. The counters and shielding actually rested on a 1/4 inch aluminum plate which could be rotated in a horizontal plane about a point which was under the center of the target holder. The target holder did not move with the counters, so the axis of the counters rotated about the center of a stationary target.

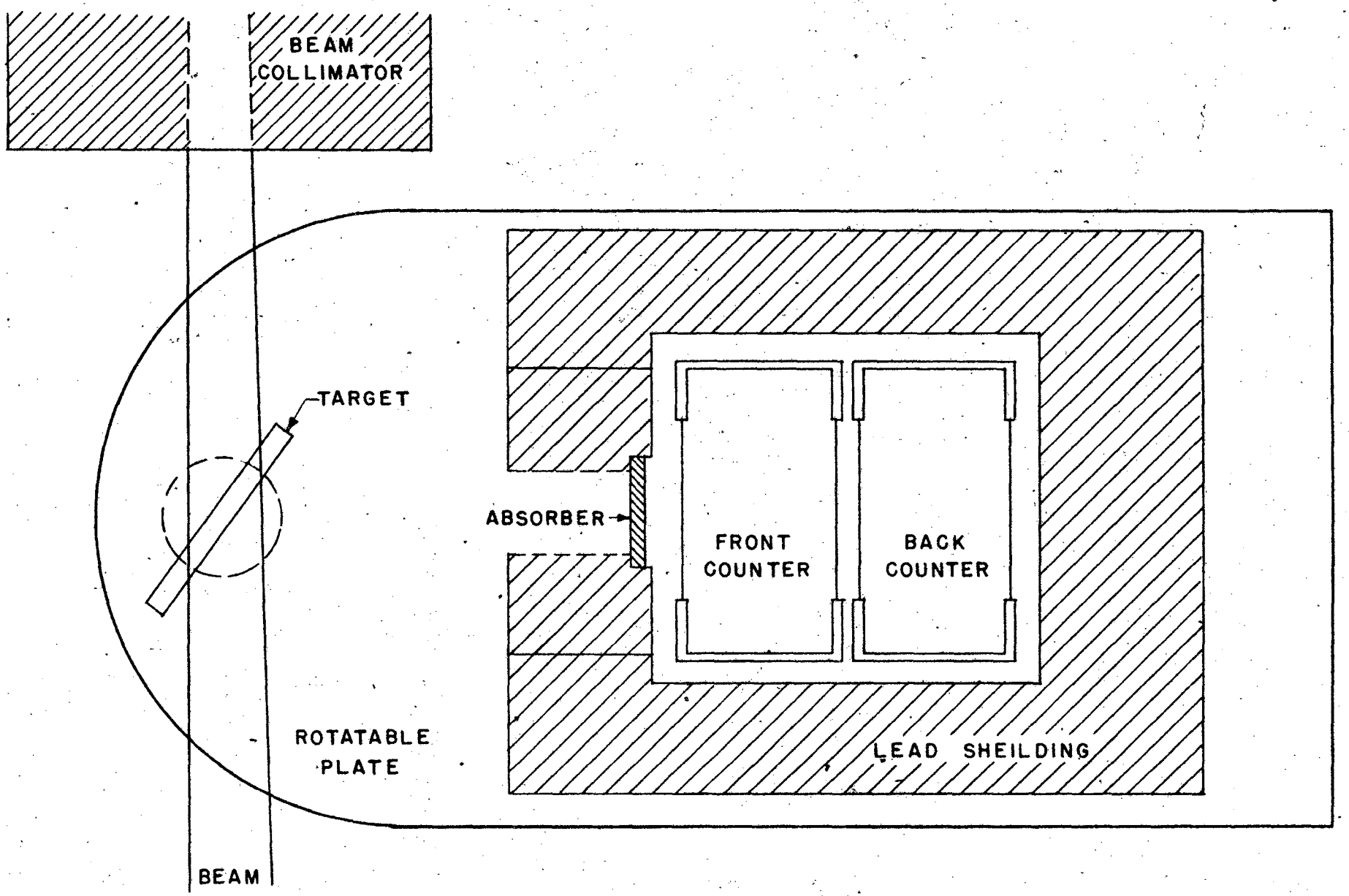

FIG. IV – (1)

14461

The synchrotron beam was collimated to a diameter of one inch by a tapered hole in a 6 inch lead block. This collimator, placed 60 inches from the platinum target of the synchrotron, passed about 40 percent of the total beam intensity according to the beam measurements made by the synchrotron crew.

In most of the runs, the target under investigation was placed 10 inches from the beam collimator, so that the beam would be spread to 7/6 inch in diameter. The fact that the beam intensity is not uniform over its one inch diameter is important in these investigations only in determing the effect of multiple scattering in the absorber and in the calculations of absolute value of the cross-section. As can be seen in Figure IV-(2) the ratio of the intensity at the center to that at a half inch radius is 2.5.

The beam was monitored by a thin walled ionization chamber constructed by Mr. Craig Nunnan and calibrated by Blocker and Kenney[23].

INTENSITY DISTRIBUTION IN SYNCHROTRON BEAM.

20 MIL PT TARGET, 335 MEV.

CURVE I : INTENSITY vs. RADIUS

CURVE II : INTENSITY × r vs. RADIUS

CURVE III : $\int_0^r$ INTENSITY × r dr vs. RADIUS

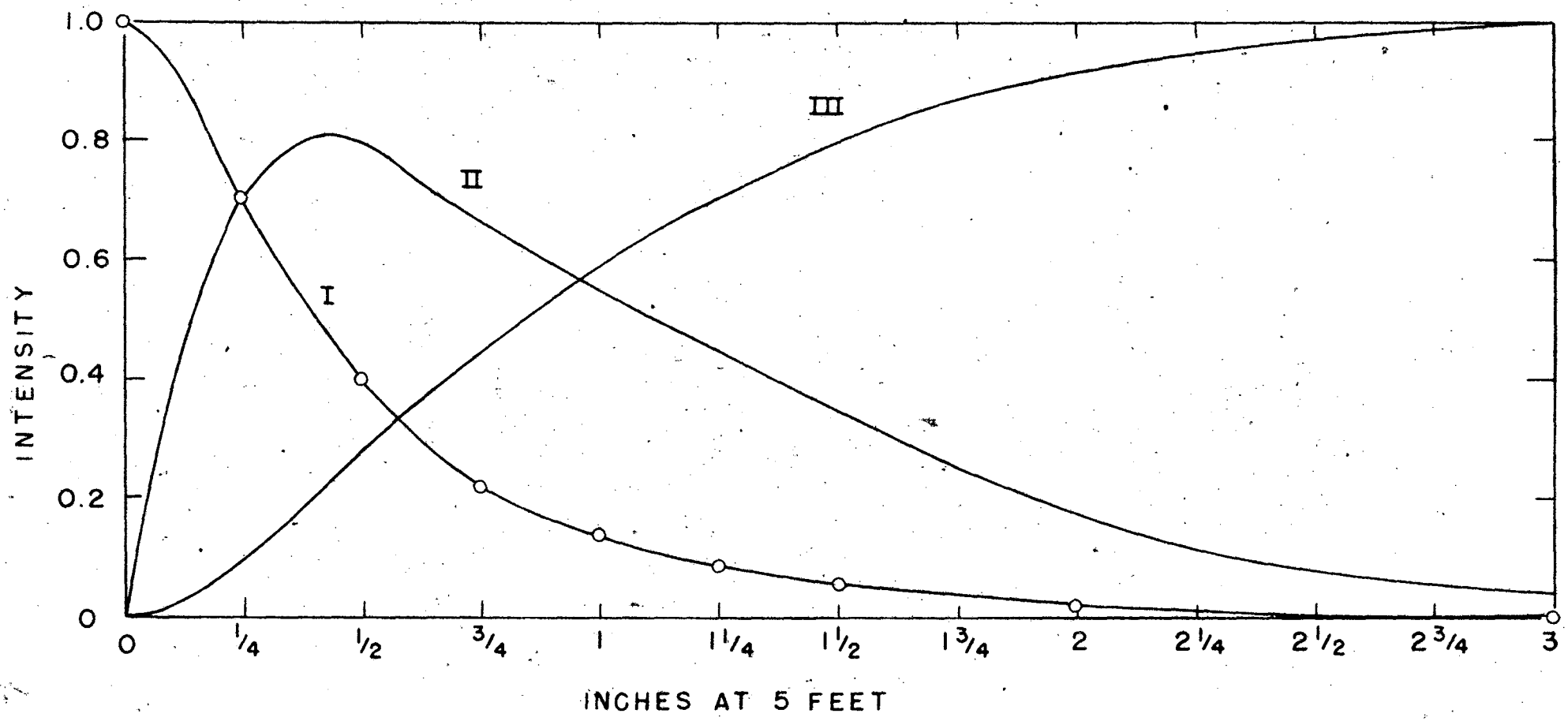

FIG. IV (2)

V Experimental Checks.

Before trying to obtain any detailed information about the protons from the gamma ray reactions it was necessary to demonstrate that the counts recorded actually represented protons coming from the target.*

Throughout this work a 1 milligram radium source was used to supply low energy electrons with which the counters could be checked. The largest pulses produced by these electrons were used as a rough standard in setting the wire voltage in the counter, the gains of the amplifiers, and the pulse height discriminators. This type of calibration is of course not very precise but it is extremely convenient and enabled resetting of the overall gain to within about 10 percent.

The first series of checks of the counter system was made with the alpha-particles from a polonium source. For this purpose a special thin window was put on one of the counters. The window was a piece of 0.00025-inch nylon covering a 1/16-inch hole in the end plate of the counter, and it allowed the 5.16 Mev alpha-particles to enter the counter. The alpha-particles were used to measure the gas multiplication of the counter as a function of the voltage on the wire. When these measurements were made, the diameter of the wire was 0.010-inch and the gas mixture was 97 percent argon and 3 percent CO_2 with a total pressure of 1/2 atmosphere.

*Target as used here and in the following means the material being bombarded by the gamma ray beam, not the platinum target in the synchrotron which produces the beam.

The assumption made for these measurements was that below 800 volts on the wire, where the output pulse height did not change, the multiplication was unity. Figure V-(1) shows the results. The crosses are the values obtained for our counters, and the solid line represents the data obtained by Diven and Rossi[24]. Their counter was cylindrical in shape with a 0.010-inch wire, and outer diameter of 0.87-inch, and filled with a 98 percent argon and 2 percent CO_2 mixture at 40 centimeters pressure. The multiplication in a cylindrical counter should be a function of

$$M = M\left[\frac{V}{\ln a/b}, Pa\right] \qquad (1)$$

where a and b are the diameter of the wire and the walls respectively; P is the gas pressure and V the voltage on the wire. The circles in Figure V-(1) show the multiplication for our counters plotted at the voltages reduced by the appropriate ratio of ln(b/a) assuming ours to be equivalent to a cylindrical counter of 4 inch diameter. It is evident that the agreement is sufficient so that the extrapolation of the data given by Diven and Rossi to the present case will give the multiplication to within a factor of 2. The voltage used in the actual experiments correspond to a multiplication of about 10. Under these conditions, the change in the amplitude of the pulse from the counter is about 1.5 percent per volt change in the counter voltage. This voltage was held constant to within 2 volts by an electronic regulator and frequent checks on a precision meter.

Table V - (1)

	Front Counter	Back Counter	Coincidence	Monitor Divisions	Time for Run (Minutes)
1/4 in. C Target; No Absorber Discriminators; Front Size 1, Back Size 2	4,249	321	256	100	5.1
Same with 4 μ Sec. Delay in Back Channel	4,493	354	0	100	6.0
No Target; No Absorber No Delay Discriminators; Same	374	287	2	100	5.5
1/4 in. C Target; No Absorber 15 ms/cm^2 Between Counters Discriminators; Front Size 2, Back Size 1	1,016	3,182	113	100	5.7
1/4 in. C Target; No Absorber 28 mg./cm^2 Between Counters Discriminators; Front Size 1, Back Size 2	6,310	423	349	100	8.4
1/4 in. C Target; No Absorber 28 ms/cm^2 Between Counters Discriminators; Front Size 2, Back Size 1	915	10,910	39	100	9.5

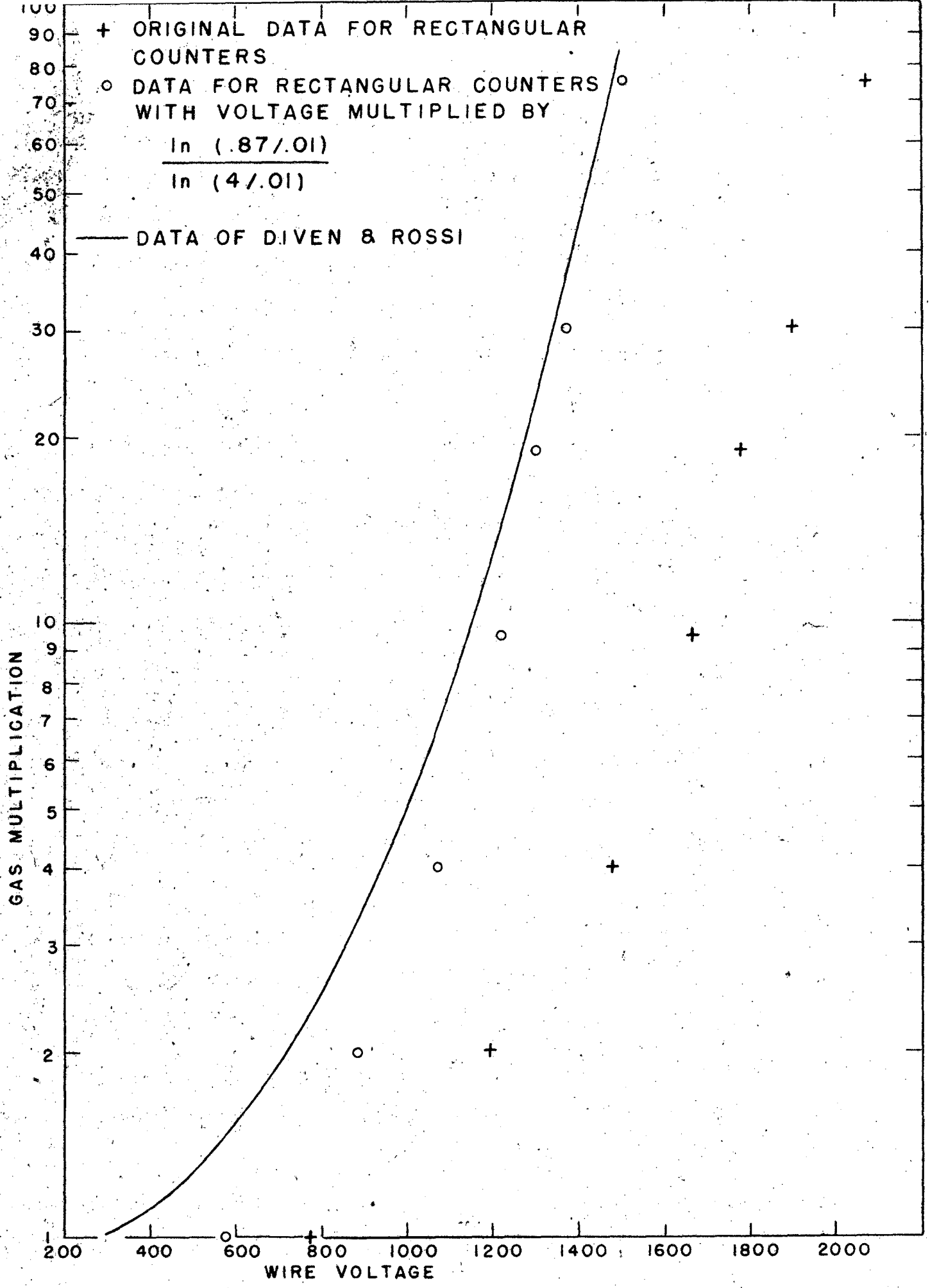
+ ORIGINAL DATA FOR RECTANGULAR COUNTERS
o DATA FOR RECTANGULAR COUNTERS WITH VOLTAGE MULTIPLIED BY
ln (.87/.01) / ln (4/.01)
DATA OF DIVEN & ROSSI
GAS MULTIPLICATION
WIRE VOLTAGE
100
90
80
70
60
50
40
30
20
10
9
8
7
6
5
4
3
2
1
200
400
600
800
1000
1200
1400
1600
1800
2000

FIG. V-(1)

In addition to the measurements of gas multiplication, the counters and electronics were checked as to dead time and coincidence resolving time. The former was done with a variable repetition rate pulse generator and the latter by measuring the accidental coincidences between two counters each bombarded by a strong beta source. The coincidence resolving time was found to be equal to the width of the gate formed by the variable gate circuit, thus indicating that the system was working properly. The dead time was just about a microsecond longer than the sum of the delay and the gate width set into the variable gate circuit. This is only slightly more than is to be expected for the recovery of the type of circuit used. The importance of the coincidence resolving time is readily understood when it is recalled that the beam from the synchrotron is pulsed. The duration of the pulse is about 2 milliseconds and there are 6 pulses per second. The beam therefore is striking the target for 1/80th of the total time. This means that the instantaneous counting rate is 80 times larger than the measured counting rate. The accidental coincidence rate is then given by

$$N_{accid} = 2\tau_r N_1 N_2 \qquad (2)$$

where $N_1 N_2$ and $N_{accid.}$ are the recorded counts per second in ~~circuit~~ #I, counter #II and the accidentals in the coincidence ~~counter~~ circuit respectively; and τ_r is the coincidence resolving time in seconds. Since for some of the data the single counting rates N_1 and N_2 were quite high and the <u>real coincidences</u> were low it was

necessary to be able to calculate the accidentals with reasonable accuracy. Actually no data were taken with the accidental coincidences more than 15 percent of the reals, so calculating the accidentals to within 20 percent meant only a 3 percent maximum uncertainty in the result.

The correction due to the time that one of the circuits is unable to respond to an incoming pulse is given by

$$f = 2\tau_d N \qquad (3)$$

where f is the fraction of the counts lost in a counter with a counting rate N and dead time τ_d. The dead time was always less than 5 microseconds, and with the maximum counting rates used this correction was less than 1 percent.

The first actual operating check of the counters was made using protons from the linear accelerator scattered from carbon. The distribution of these protons has been studied using photographic plates[25], and it is known that the first excited state of C^{12} is at 4.6 Mev. Therefore the protons elastically scattered at 90° should have 4.25 Mev more energy than the first inelastically scattered group. The counting rate vs. absorber thickness (in mils of aluminum) is shown in Figure V-(2). For this experiment only a single counter was used and the pulse height discriminator was biased so that only pulses 4 times as high as the largest from the radium source were counted. It is clear from the results that protons passing through the counter with more than a few mils residual range did not produce large enough pulses to count. From the width of the

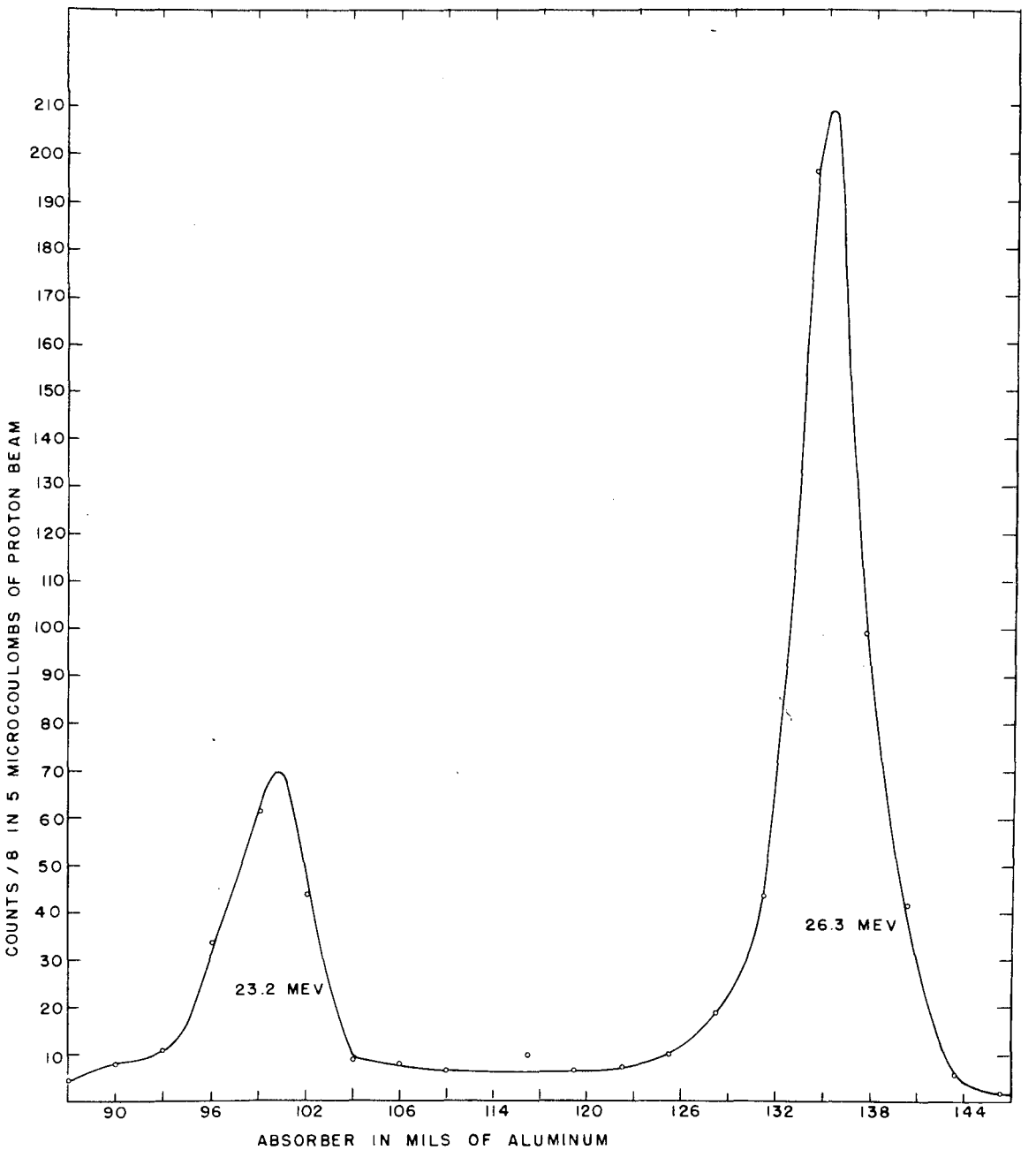
COUNTS / 8 IN 5 MICROCOULOMBS OF PROTON BEAM
210
200
190
180
170
160
150
140
130
120
110
100
90
80
70
60
50
40
30
20
10
23.2 MEV
26.3 MEV
90
96
102
106
114
120
126
132
138
144
ABSORBER IN MILS OF ALUMINUM

peaks we can say that the range interval counted was certainly less than 2 mils of aluminum.

It was expected that the background of electrons near the synchrotron beam would make counting protons very much more difficult than it had been at the linear accelerator. However, this was not entirely so. The electron background was somewhat troublesome, but it did not lead to an appreciable amount of piling up of electrons in the half microsecond times involved in one pulse. Neglecting for a moment the problem of multiple electron production, i.e. showers, it is clear that one can select the large pulses due to protons without counting any electrons by running at sufficiently low beam intensities. The only real problem was whether one could count protons at a reasonable rate and still not be bothered by electrons. This was demonstrated in the first few runs by a series of checks.

For the following discussion let us call the height of the largest pulses from the radium source unity and designate the smallest pulses counted in any counter on this scale. The first count was taken with a 1/4-inch carbon target and the two counters set at 90° to the beam direction. The biases were adjusted so that the first counter accepted pulses of height 1, and the second pulses of height 2; with no absorber in front of the counters this gave a coincidence counting rate of 51 counts per minute with the best beam available. At the same time the front counter had a rate of 850 counts per minute and the back counter 70 counts per minute. The calculated accidental counting rate was 0.07 counts per minute

and with a 4 microsecond delay introduced in one channel, no coincidences were recorded in 5 minutes. With the target removed, the coincidence rate went down to about 0.5 counts per minute. Then with the target in place and a total of 15 mg/cm^2 of aluminum between the counters the amplifier gains were changed so that the first counter accepted size 2 pulses and the back counter size 1. The counting rate was then down to 20 counts per minute. At a later time this was done with 28 mg/cm^2 of aluminum between the counters and the counting rate was less than 7 count per minute. With a 2-inch lead absorber in front of the counters the coincidence rate also went to less than 1 count per minute. From this data several conclusions can be drawn. First, the counts were due to particles coming directly from the target; second, they are heavy particles near the end of their range; third, the range interval counted is equivalent to about 30 mg/cm^2 of aluminum.

The fact that electrons are not producing the coincidences can be understood by considering the only events in which electrons could produce counts. The discriminators are set so that a single electron will not produce a count in the back counter and will count in the front counter only if it just stops in it. However, there is sufficient material between the counters so that if an electron produces a large pulse in one counter it will be very close to minimum ionization in the other and will produce a pulse of about 1/5 unit amplitude. Therefore, for electrons to produce a coincidence, 2 of them must stop in the back counter and another in the front

counter, all within a time of 4×10^{-7} seconds. Furthermore, if this event did happen, it would be just as likely that 2 electrons would stop in the front counter and 1 in the second; but when the gains are reversed, this is not found to be so.

The counting rate was also checked as the beam intensity was reduced. The beam was reduced by as much as a factor of 5, and the coincidence counting rate was always proportional to the beam, and not to the square of the beam as it would be if accidental pile-up were involved. The results of these checks are summarized in the typical data given in Table V-(1).

Finally, the distribution in amplitude of the pulses in the first counter was determined for those pulses which were accompanied by counts in the second counter. The electronic system for this measurement was discussed in section III and the results are given in Figure V-(3).

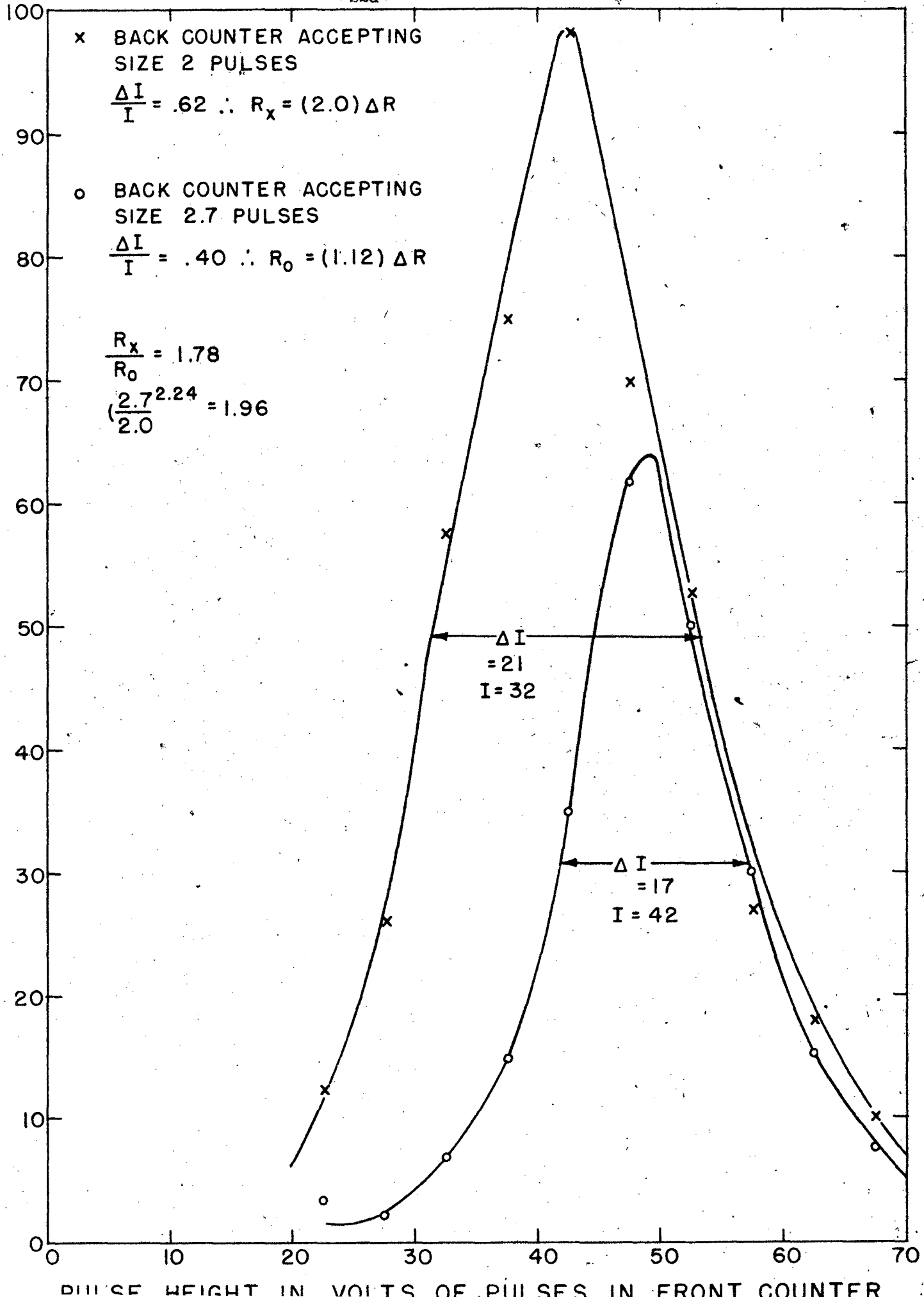
× BACK COUNTER ACCEPTING SIZE 2 PULSES
$\frac{\Delta I}{I} = .62 \therefore R_x = (2.0)\Delta R$
o BACK COUNTER ACCEPTING SIZE 2.7 PULSES
$\frac{\Delta I}{I} = .40 \therefore R_0 = (1.12)\Delta R$
$\frac{R_x}{R_0} = 1.78$
$(\frac{2.7}{2.0})^{2.24} = 1.96$
ΔI = 21
I = 32
ΔI = 17
I = 42
0
10
20
30
40
50
60
70
80
90
100
PULSE HEIGHT IN VOLTS OF PULSES IN FRONT COUNTER

VI Calculations and Corrections:

The measurements made in these experiments give the distribution range of the protons and the energy distribution must be inferred from these data.

We can consider the target surrounded on all directions by a sea of material in which the counter system records all the protons that come to rest in a certain solid angle and in a small interval of range. This interval of range is calculated as described in Section II from the data such as are given in Figure V-(3). In all of the runs it was approximately equal to 30 mg/cm^2 of aluminum. In practice, of course, the counters are not moved but are kept fixed in space and varying thicknesses of absorber are placed in front of them.

In addition to the interval in range accepted by the counters there is an uncertainty in range due to the finite thickness of the target. Since the counting rates are generally quite low it is necessary to use as thick a target as is reasonable. However, reasonableness in this connection must be considered in terms of the energy distribution which is ultimately to be calculated. Differentiating Equation II-(4), we have:

$$\frac{\Delta R}{R} = 1.8 \frac{\Delta E}{E} \qquad (1)$$

For the energy distributions $\Delta E/E$ was held between 10 and 30 percent so $\Delta R/R$ could be between 18 and 54 percent.

The final result of the calculations is the determination of the differential cross section for the photo-ejection of protons of energy E at an angle θ. We write this quantity as $\frac{d\sigma}{dE d\Omega}(E,\theta)$ which will be abbreviated to $d\sigma(E,\theta)$.

The differential cross section is given by

$$d\sigma(E,\theta) = \frac{N_p(E,\theta)}{N_{in}(N_t/cm^2)\Delta E \ \Delta\Omega}$$

where $N_p(E,\theta)$ is the number of protons counted at the energy E, and angle θ; ΔE is the energy region accepted by the counting system and $\Delta\Omega$ the solid angle subtended at the target by the opening to the counting system. N_t/cm^2 is the number of target nuclei per cm^2 as seen by the beam; and N_{in} is the number of gamma rays incident on the target. At least some degree of arbitrariness is involved in the definition of N_{in} because of the nature of the Bremsstrahlung beam. For the first of these calculations N_{in} will be taken as the number of "effective quanta" by which we mean the total energy in the beam in Mev divided by the maximum energy of 335 Mev.

ΔE is equal to dE/dx (in $Mev/mg/cm^2$) multiplied by the range interval ΔR, which equals 30 mg/cm^2 as mentioned above, accepted by the counters. The rate of energy loss, dE/dx, is that for the protons as they leave the target. The absolute error in ΔR as obtained from the pulse height distribution is probably less than 25 percent but this error is difficult to evaluate; and the same statement of error applies to the solid angle. However, N_p, the relative value of N_{in} and

N_t/cm^2 are known to about 3 percent. Therefore the absolute value of the cross section may be in error by as much as a factor of two, but the relative cross sections have errors which are determined primarily by the counting statistics since the large errors mentioned do not effect relative cross section calculations.

For the low energy region of the energy distribution where very thin targets must be used, the no-target background becomes significent. Considerable effort went into attempts to reduce this source of background, but the best that could be achieved was a no-target background equivalent to about 15 percent at the 9.4 Mev point.

In addition to the accidental coincidence correction which was mentioned above there are two other sources of error which must be considered. These are; first, the effect of nuclear absorption in the absorber; and second, the multiple scattering in the absorber. The correction for nuclear absorption can be made quite simply. If we take the geometrical cross section for the absorption, the fraction of the protons absorbed is about 9 percent per centimeter of copper absorber. Thus for the highest energy point taken this effect produces a correction of about 6 percent.

The effect of multiple scattering is more difficult to evaluate with accuracy. Scattering which takes place in the material between the two counters cannot cause any error except for very large scattering angles, and this effect has been ignored. The root mean square scattering angle of the particles as they enter the first counter can be obtained from the calculations of R. R. Wilson [26]. The formula

given by Wilson is plotted in Figure VI-(1). The maximum value of the fraction of the range traversed before entering the first counter was 0.98, and since the portion of the absorber close to the counter was always aluminum, the maximum value of θ r.m.s. was 0.11 radians.

The effect of the scattering was calculated after making the following simplifying assumptions: 1) the probability of scattering into an angle θ is taken as a gaussian function of θ; 2) the problem is treated as though it were two dimensional; 3) a rough numerical integration was made by dividing the target into three zones as shown in Figure VI-(2). This correction was 6 percent of the high energy point, and was not made since it is small and not accurately known. At all lower energy points this correction is certainly negligible as can be seen from the way θ r.m.s. falls with decreasing (x/R) in Figure VI-(1).

Angular Distributions.

The angular distributions were taken with the target fixed and the counters rotated about the center of the target. The ratio of the counts at two angles was measured in successive runs. For these measurements the target was fixed with the normal to its surface bisecting the angle made by the two counter positions; in this way the target presented the same aspect to the counters in both runs. This procedure eliminated all corrections in the angular distributions and the ratio of the $d\sigma(E,\theta)$ at the two angles was just the ratio of the counts divided by the reading on the beam monitor.

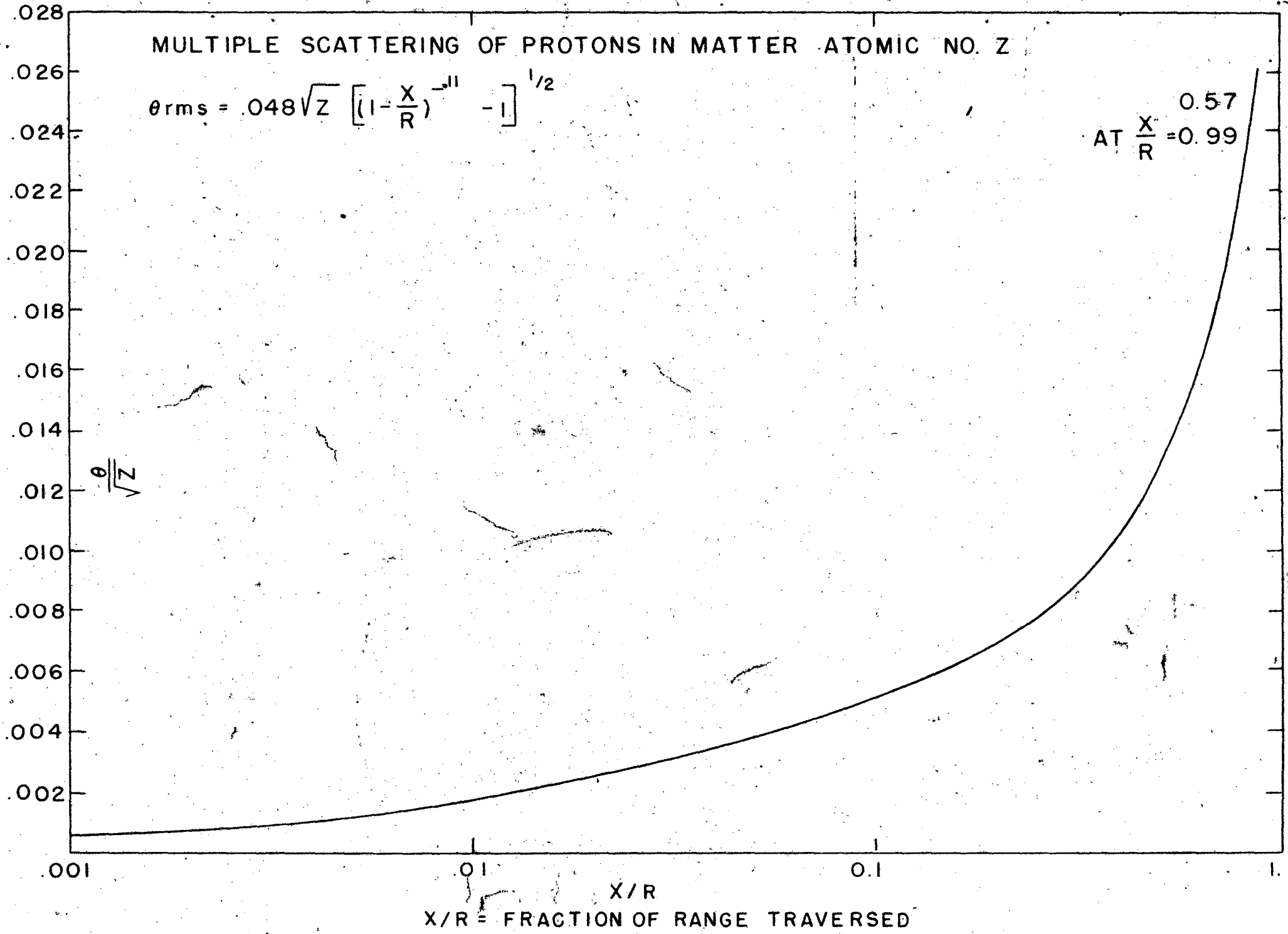
MULTIPLE SCATTERING OF PROTONS IN MATTER ATOMIC NO. Z
θrms = .048√Z [(1-X/R)^-.11 - 1]^1/2
0.57
AT X/R =0.99
θ/√Z
.028
.026
.024
.022
.020
.018
.016
.014
.012
.010
.008
.006
.004
.002
.001
.01
0.1
1.
X/R
X/R = FRACTION OF RANGE TRAVERSED

FIG. VI (1)

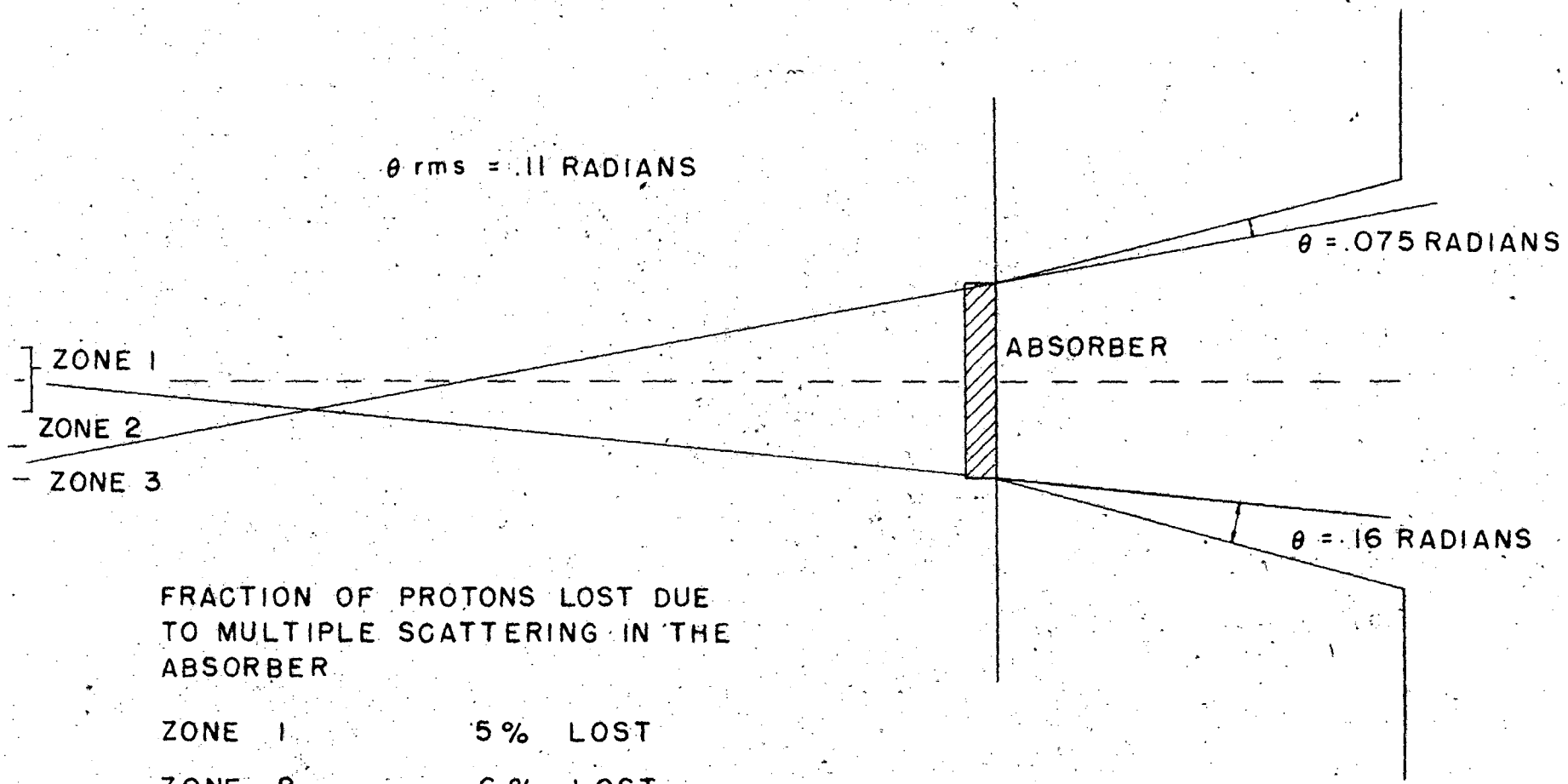

FRACTION OF PROTONS LOST DUE TO MULTIPLE SCATTERING IN THE ABSORBER

ZONE 1	5 % LOST
ZONE 2	6 % LOST
ZONE 3	8 % LOST

TOTAL CORRECTION 6 PERCENT

SIMPLIFIED GEOMETRY FOR CALCULATING EFFECT OF MULTIPLE SCATTERING

FIG. VI (2)

VII Results and Discussion.

The averages of the results of the energy distributions are given in Table VII-(1). As stated above, the accuracy of the relative values of all of the data are limited only by the statistical errors (given throughout as standard errors), and the corrections due to multiple scattering. The absolute values of all of the cross sections are believed to be correct to within about a factor of two. The distributions for each of the three elements measured are shown in Figure VII-(1), with the cross sections for each element divided by the 2/3 power of the atomic number. It can be seen that the data for lead begins to deviate from the trend in carbon and copper at about 13 Mev. This decrease in yield from lead at low energy is to be expected because of the coulomb barrier which is 13.7 Mev. The fact that this effect of the barrier appears at about the correct energy is further evidence that we are counting protons.

To show the form of the energy distributions, they are plotted on log-log paper in Figures VII-(2), (3), and (4). Except for the effect of the coulomb barrier in lead, the data are all consistent with the best fit straight lines shown. Thus the yields are proportional to $1/E^s$ where s is $2.2 \pm .2$ for lead, $1.9 \pm .1$ for copper, and $1.7 \pm .1$ for carbon. The differences seem to be beyond experimental error but not enough that very much significence can be attributed to them.

The angular distributions consist only of three angles for carbon, and four for copper. All of these measurements covered an

Table VII - (1)

CARBON

E To Target Center (Mev)	E Minimum in Mev	E Maximum in Mev	$\frac{d\sigma(E, \pi/2)}{dEd\Omega}$ in cm^2/Mev Steradian	$\frac{d\sigma(E, \pi/2)}{A^{2/3}dEd\Omega}$	Standard Error Percent
8.7	6.6	10.7	9.2×10^{-30}	17.1×10^{-31}	4
12.2	10.8	13.6	5.2	9.6	6
19.1	17.7	20.5	2.76	5.12	10
33.5	31.1	34.8	.88	1.65	12
41.5	32.3	50.	.644	1.19	6
54.	48.	60.	.490	.91	12
67.	62.	72.	.272	.50	15

Table VII - (1) - Continued

COPPER

E to Target Center (Mev)	E Minimum in Mev	E Maximum in Mev	$\frac{d\sigma(E, \pi/2)}{dE d\Omega}$ in cm^2/Mev Steradian	$\frac{d\sigma(E, \pi/2)}{A^{2/3} dE d\Omega}$	Standard Error Percent
9.5	7.25	11.4	$47. \times 10^{-30}$	29.6×10^{-31}	4.4
14.9	13.3	16.2	16.9	10.6	8.5
20.2	18.0	22.1	9.9	6.2	8.0
29.0	26.2	31.6	4.8	3.0	11.5
40	32.3	47.0	2.85	1.79	5.3
68	62.0	73.8	0.94	.59	14.

Table VII - (1) - Continued

LEAD

E to Target Center (Mev)	E Minimum in Mev	E Maximum in Mev	$\frac{d\sigma(E, \pi/2)}{dE d\Omega}$ in cm^2/Mev Steradian	$\frac{d\sigma(E, \pi/2)}{A^{2/3} dE d\Omega}$	Standard Error Percent
9.4	7.25	11.4	35.2×10^{-30}	$93. \times 10^{-32}$	7.4
12.5	10.7	14.1	43.1	113.	6.4
19.1	17.8	20.2	31.0	81.	11.
25.0	22.3	27.6	19.9	53.	10.
34.3	32.3	36.3	10.2	26.1	15.
40.0	32.3	47.0	8.0	21.0	4.5
67.5	62	72.2	2.0	5.4	15.

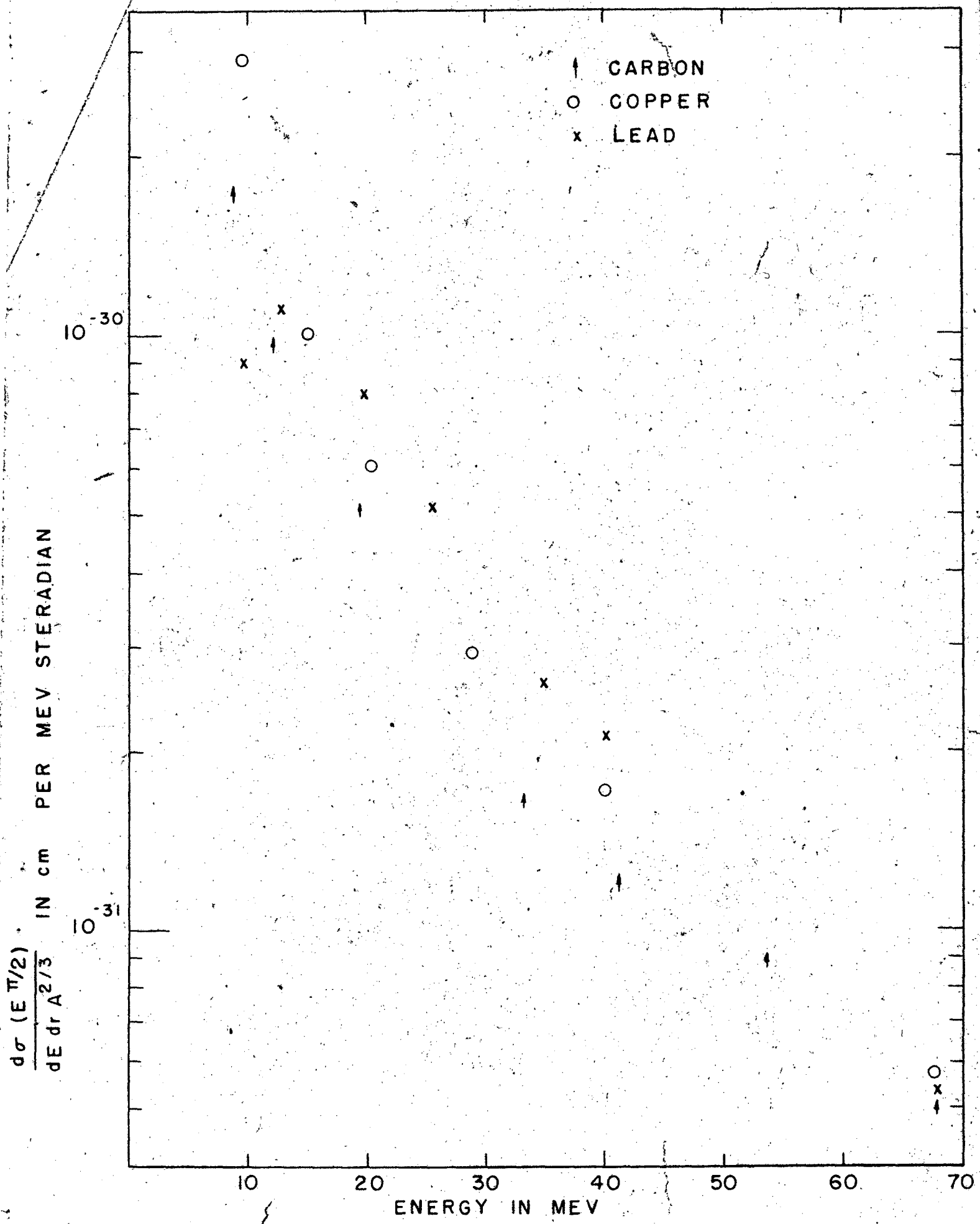
CARBON
COPPER
LEAD
10^{-30}
10^{-31}
$\frac{d\sigma}{dE\,dr}\,(E^{\pi/2})\,A^{2/3}$ IN cm PER MEV STERADIAN
10
20
30
40
50
60
70
ENERGY IN MEV

FIG VII (1)

PRINTED IN U.S.A. ON CLEANPRINT TECHNICAL PAPER NO. 1666H
TECHNICHART

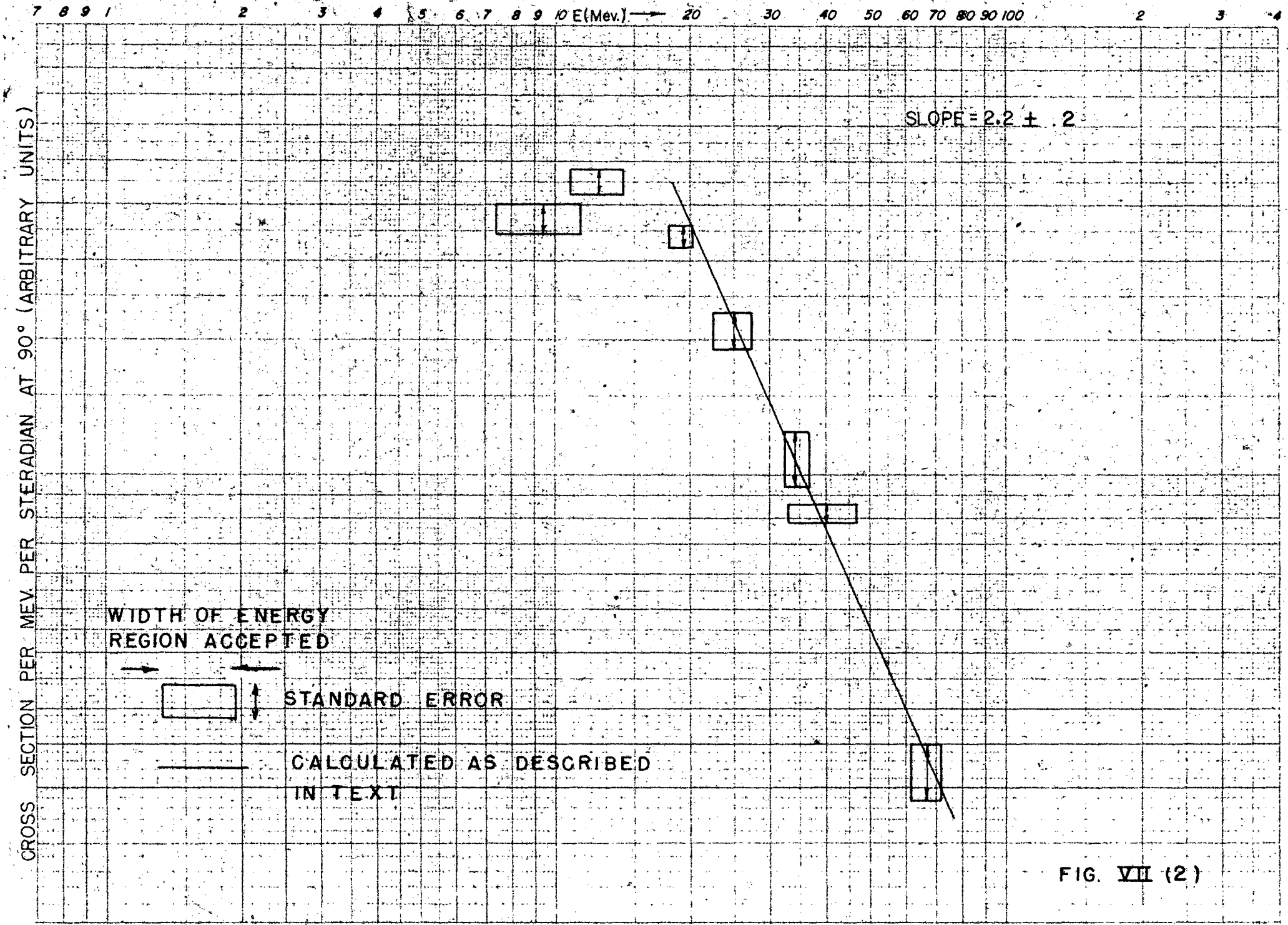

FIG. VII (2)

ENERGY DISTRIBUTION OF PROTONS EJECTED FROM LEAD BY SYNCHROTRON BEAM

14475

CLEARPRINT PAPER NO. T323 LOGARITHMIC 2¼ BY 2 3¼ INCH CYCLES
PRINTED IN U.S.A. ON CLEARPRINT TECHNICAL PAPER NO. 1000H

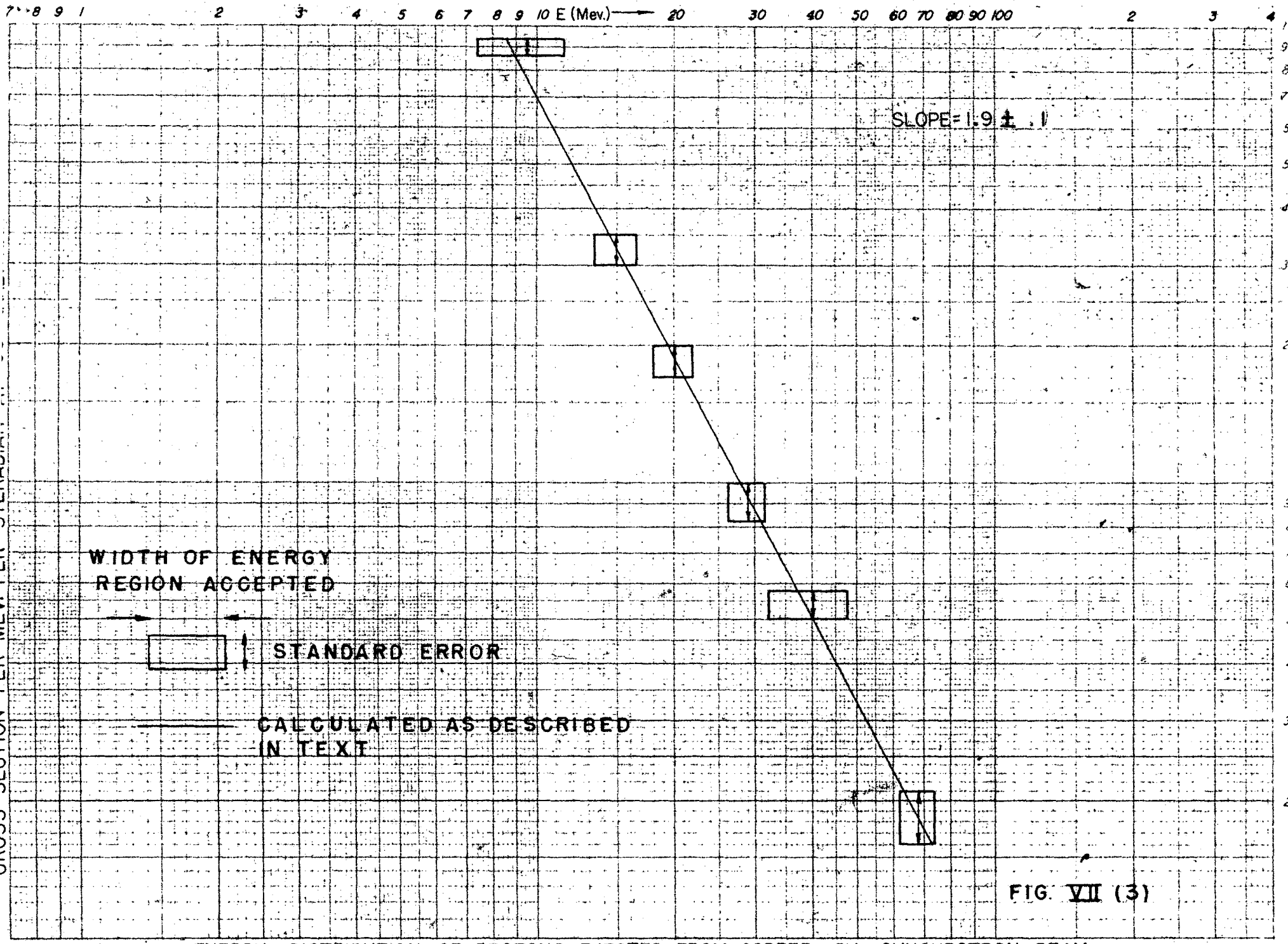

FIG. VII (3)

ENERGY DISTRIBUTION OF PROTONS EJECTED FROM COPPER BY SYNCHROTRON BEAM

14473-1

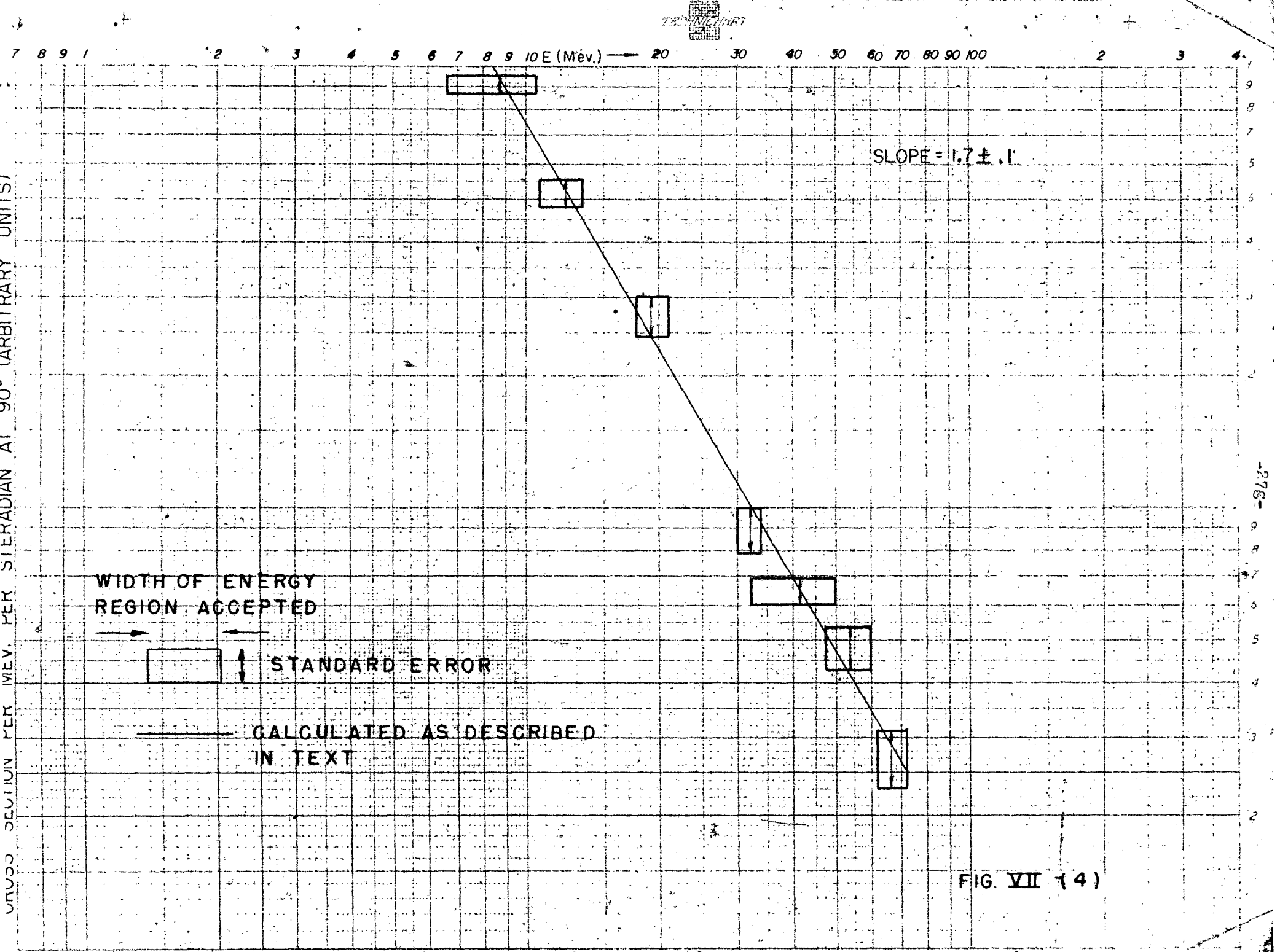

FIG. VII (4)

ENERGY DISTRIBUTION OF PROTONS EJECTED FROM CARBON BY SYNCHROTRON BEAM

14474

energy region of 25 to 38 Mev. The relative yields, normalized to 90°, are as follows:

	Copper		Carbon	
45°	1.31	.09	1.25	.09
67°	1.50	.13	———	
90°	1.00 (by definition)		1.00	
135°	0.70	.04	0.58	.04

We shall now attempt to show that the data obtained in these experiments suggest the direct photo-effect as the mechanism for the (γ,p) reactions. This means that the gamma ray interacts primarily with a single proton and does not deliver its energy to the nucleus as a whole. Interaction with a single particle is immediately suggested by the angular distributions as it is difficult to imagine how a compound nucleus effect could produce the pronounced forward peak which is observed. If we consider a single particle interaction, then the forward peak will be explained at least in part as due to the aberration of the angle of incidence of the gamma ray as seen by the rapidly moving proton. The relativistic transformation of the angles is given by[2]

$$\cos\theta = \frac{\cos\theta' + \beta}{1 + \beta\cos\theta'} \qquad (1)$$

where θ is the angle between the direction of the protons' motion and the beam in the laboratory system, θ' is this angle in the proton's system, and β is the velocity of the proton divided by the velocity of light. From Equation (1) it follows that the solid angle $d\Omega$, which is proportional to $\sin\theta\, d\theta$, transforms as

$$d\Omega = \frac{d\Omega'}{(1 + \beta\cos\theta')^2} \qquad (2)$$

Applying these transformations to our data with $\beta = .26$ for a 30 Mev proton we obtain the following:

θ proton's system	$d\sigma'/d r' d E$	
	Copper	Carbon
57°	$.93 \pm .07$	$.89 \pm .03$
105°	1.00	1.00
144°	$1.04 \pm .06$	$0.86 \pm .06$

These results indicate symmetry about 90° to within the accuracy of the experiment. Such symmetry is to be expected if we consider only the classical electro-magnetic interaction of the gamma ray and a single proton.

The energy distribution and the absolute value of the cross section also support the idea of a photo-effect. If we consider the calculations for the photo-disintegration of the deuteron, we have for the energy dependent term[28]

$$d\sigma(E) \sim \frac{y^{3/2}}{(1+y)} \qquad y = \frac{E_{binding}}{E} \tag{3}$$

where $E_{binding}$ is the binding energy of the proton to the nucleus which we can take as about 8 Mev, and E is the energy of the proton as it leaves the nucleus. This type of process implies a connection between the energy of the proton and that of the photon which caused the ejection. When a particle is pulled out of a nucleus in this fashion there is not sufficient time for the rearrangement to the ground state wave function of the residual nucleus. Calculations of the energy necessary in such a non-adiabatic process have not been done, but the experiments of York[29] with high energy

neutrons indicate that about 12 Mev will be left in the nucleus.

The number of photons of energy (E + 20) Mev multiplied by Equation (3) is plotted in Figure VII-(5), along with the energy distribution from copper. The curve was normalized to fit the data at 30 Mev, and it can be seen that the agreement is quite good in the high energy region. If this explanation of the results is correct, the disagreement at low energies can be explained either by the crudeness of the model taken in the calculations or as due to the neglect of the expected low-energy protons from the compound nuclei in which the gamma ray energy has been completely observed.

The absolute value of the cross section obtained from these calculations is approximately

$$d\,\sigma\,(E,\theta) = \left(\frac{e^2}{\hbar\, c}\right) \sigma \text{ geometrical } \frac{y^{3/2}}{(1+y)^3} \sin^2\theta \qquad (4)$$

This result is obtained from the Bethe Peierls calculations of the photo-disintegration of the deuteron together with the assumption that only those protons at the surface can be successfully ejected by a gamma ray. The value obtained from Equation (4) multiplied by the number of gamma rays of energy (E + 20) per equivalent quanta (using the Bremsstrahlung spectrum given by Heitler[30]) is in surprisingly good agreement with the the results given in Table VII-(1). For instance, for lead at 40 Mev, and at 90°, equation (4) gives $d\,\sigma(40\,\frac{\pi}{2}) = 1.7 \times 10^{-29} cm^2$, while the observed value is $d\,\sigma = 8 \times 10^{-30} cm^2$.

It should be noticed that this type of nuclear photo-effect is not primarily a high energy phenomenon. For the energies considered here the wave length of the photons is long compared to the 'size' of a nucleus.

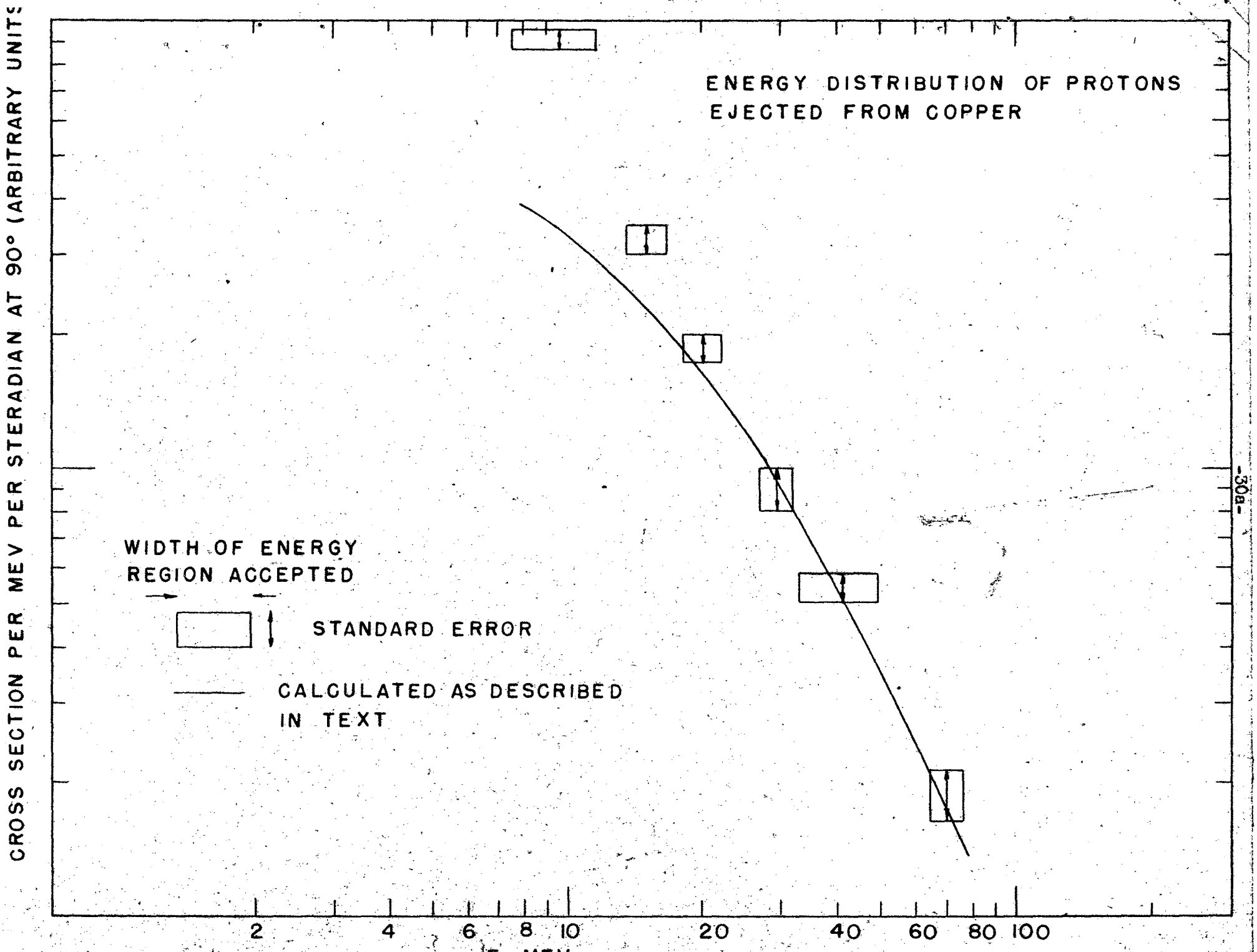
ENERGY DISTRIBUTION OF PROTONS
EJECTED FROM COPPER
CROSS SECTION PER MEV PER STERADIAN AT 90° (ARBITRARY UNITS)
WIDTH OF ENERGY
REGION ACCEPTED
STANDARD ERROR
CALCULATED AS DESCRIBED
IN TEXT
2
4
6
8
10
20
40
60
80
100
E MEV

FIG VII (5)

A particular proton is selected for ejection because it has the appropriate momentum componants when the photon strikes. Thus a further study of this process both theoretically and experimentally might yield information about the momentum distribution of particles in the nucleus.

VIII Acknowledgements.

I wish to express my graditude to Professors A. C. Helmholz and W. K. H. Panofsky for their very helpful advice and encouragement throughout this work. My sincere thanks also go to the entire synchrotron crew under the able direction of Mr. Walter Gibbons. Finally, I wish to thank Dr. A. Silverman for his valuable cooperation in all phases of this investigation. This work was sponsored by the Atomic Energy Commission.

IX Bibliography

1. Chadwick and Goldhaber, Proc. Roy. Soc. 151, 479 (1935).

2. Russell, Sachs, Wattenberg and Fields, Phys. Rev, 73, 545 (1948).

3. (a) Bethe and Genther, Zeits f. Physik 106, 236 (1937) and Zeits f. Physik 112, 45 (1939).

   (b) Huber, Lienhard and Wäffler, Helv. Phys. Acta 17, (1945).

4. Perlman and Friedlander. Phys. Rev., 74 442 (1948).

5. Bohr, Nature 137 344 (1936).

6. Weisskopf, Phys. Rev. 52, 295 (1937).

7. Feshbach and Weisskopf, Phys. Rev. 76 1550 (1949).

8. Wäffler and Hirzel, Helv. Phys. Acta 21 200 (1948).

9. Schiff, Phys. Rev. 73 1311 (1948).

10. Goldhaber and Teller, Phys. Rev. 74 1046 (1948).

11. Baldwin and Klaiber, Phys. Rev. 73 1156 (1948).

12. Heitler, The Quantum Theory of Radiation, Oxford University press, 1944, page 119.

13. Bethe and Peierls, Proc. Roy. Soc. A 148 146 (1935).

14. Rose and Goertzel, Phys. Rev. 72 749 (1947).

15. Guth and Mullin, Phys. Rev. 76 234 (1949).

16. Livingston and Bethe, Rev. Mod. Phys. 9 245 (1937).

17. Arch, Hoffman and Williams, UCRL Report Number.

18. Healey and Reed, The Behavior of Slow Electrons in Gases, Amalgamated Wireless Ltd., Sidney (1941).

19. Cerson and Wilson, Rev. Sci. Inst. 19 207 (1948).

20. Rossi and Staub, Ionization Chambers and Counters, McGraw Hill Book Co. 1949.

21. Brode, Rev. of Mod. Phys. 5, 257 (1933).

22. Elmore and Sands Electronics McGraw-Hill Book Co (1949) page 241.

23. Blocker, Kenney and Panofsky, UCRL Report Number 565.

24. Diven and Rossi, MDDC 282, 1944.

25. Levinthal, Martinelli and Silverman, Phys. Rev., in press.

26. Wilson, Phys. Rev. 71 385 (1947).

27. Smythe, Static and Dynamic Electricity, N. Y., McGraw-Hill, 1939 Page 504.

28. Bethe and Bacher, Rev. Mod. Phys., 8 83 (1936).

29. York, UCRL Report Number 359.

30. Heitler, The Quantum Theory of Radiation, Oxford University Press 1944 (page 170).